Algebraic intersection, lengths, and Veech surfaces

Julien Boulanger

Algebraic intersection, lengths and Veech surfaces

Julien Boulanger

September 29, 2023

1 Introduction

In this paper, we continue the study of intersections of closed curves on translation surfaces, initiated in [CKM21a] and [CKM21b] for a family of arithmetic Veech surfaces and [BLM22] for a family of non-arithmetic Veech surfaces. Namely, we investigate the question of maximizing the algebraic intersection between two curves of given lengths. A suitable way of quantifying this is to consider the following quantity, defined for any closed oriented surface X with a Riemannian metric g (possibly with singularities):

$$\mathrm{KVol}(X) := \mathrm{Vol}(X,g) \cdot \sup_{\alpha,\beta} \frac{\mathrm{Int}(\alpha,\beta)}{l_g(\alpha) l_g(\beta)}, \tag{1}$$

where the supremum ranges over all piecewise smooth closed curves α and β in X, Int denotes the algebraic intersection, and $l_g(\cdot)$ denotes the length with respect to the Riemannian metric (it is readily seen that multiplying by the volume $\mathrm{Vol}(X,g)$ makes the quantity invariant by rescaling the metric g). As shown by Massart-Müetzel [MM14], this function is well defined and finite.

Though KVol is a close cousin of the systolic volume $\mathrm{SysVol}(X) = \sup_\alpha \frac{\mathrm{Vol}(X)}{l_g(\alpha)^2}$, it is difficult to compute on a given surface outside the case of a flat torus (where $\mathrm{KVol} = 1$). In this context, Cheboui, Kessi and Massart [CKM21a, CKM21b] initiated the study of KVol on translation surfaces, which are instances of flat surfaces with conical singularities. More precisely, [CKM21a] provides estimates of KVol on the Teichmüller curves associated with a family of arithmetic translation surfaces (X,ω). In Boulanger–Lanneau–Massart [BLM22], we give a closed formula for KVol on the Teichmüller disk of the double regular n-gon translation surface for $n \geq 5$ odd. In this paper, we continue the study of KVol in the Teichmüller disk of translation surfaces coming from regular polygons. Namely, we deal with the case of the regular n-gon for $n \geq 8$ even. Although similar to the case of the double regular n-gon for odd n, the case of the regular n-gon for even

n requires a more careful study.

Given an even integer $n \geq 8$, we denote by X_n the translation surface made from a regular n-gon by identifying its parallel opposite sides by translations. The resulting surface has a unique conical singularity if $n \equiv 0 \mod 4$ and two distinct conical singularities if $n \equiv 2 \mod 4$. This surface can also be obtained by the unfolding construction of Katok–Zemlyakov [ZK76] from a triangle of angles $(\frac{\pi}{2}, \frac{\pi}{n}, \frac{(n/2-1)\pi}{n})$ and is one of the original Veech surfaces (see [Vee89]). As it will be recalled in Section 2, the Veech group of X_n has a *staircase model* $\mathcal{S}$ in its Teichmüller disk whose Veech group Γ_n is an index two subgroup of the Hecke group of order n. In particular, the Teichmüller curve associated to X_n can be identified with $\mathbb{H}^2/\Gamma_n$ and has a fundamental domain $\mathcal{T}_n$ depicted in Figure 1, where $\Phi := \Phi_n = 2\cos(\frac{\pi}{n})$.

In this paper, we study KVol in the Teichmüller disk of X_n, and we give a formula to compute KVol on any surface of $\mathcal{T}_n$ for $n \equiv 0 \mod 4$. If $n \equiv 2 \mod 4$, the fact that X_n has two singularities makes it more difficult to compute KVol. In this latter case, our methods provide upper bounds on KVol in the Teichmüller disk of X_n.

The case $n \equiv 0 \mod 4$. Our main result holds in the case where $n \equiv 0 \mod 4$, so that the regular n-gon as a single singularity, and can be stated as:

Theorem 1.1. *Let $n \geq 8$ such that $n \equiv 0 \mod 4$. Given $d, d' \in \mathbb{R} \cup \{\infty\} \simeq \partial\mathbb{H}^2$, let $\gamma_{d,d'}$ denote the geodesic in the hyperbolic plane $\mathbb{H}^2$ having d and d' as endpoints, and define:*

$$\mathcal{G}_{max} = \bigcup_{k \in \mathbb{N}^* \cup \{\infty\}} \gamma_{\infty, \pm\frac{1}{k\Phi}}$$

(with the convention $\frac{1}{\infty} = 0$).

Let $X = M \cdot \mathcal{S}_n$ be a surface in the Teichmüller disk of X_n, obtained from the staircase model $\mathcal{S}$ by applying a matrix $M = \begin{pmatrix} a & b \\ c & d \end{pmatrix} \in SL_2(\mathbb{R})$. Then, we have:

$$\mathrm{KVol}(X) = K_0 \cdot \frac{1}{\cosh(\mathrm{dist}_{\mathbb{H}^2}(\frac{di+b}{ci+a}, \Gamma_n \cdot \mathcal{G}_{max}))} \tag{2}$$

Where $K_0 > 0$ is an explicit constrant which only depends on n and $\mathrm{dist}_{\mathbb{H}^2}$ denotes the hyperbolic distance.

In particular, KVol is bounded on the Teichmüller disk of the regular n-gon, and

(i) the maximum of KVol is achieved for surfaces represented by images of elements of $\mathcal{G}_{max}$ under the group Γ_n,

(ii) the minimum of KVol is achieved, uniquely, at X_n.

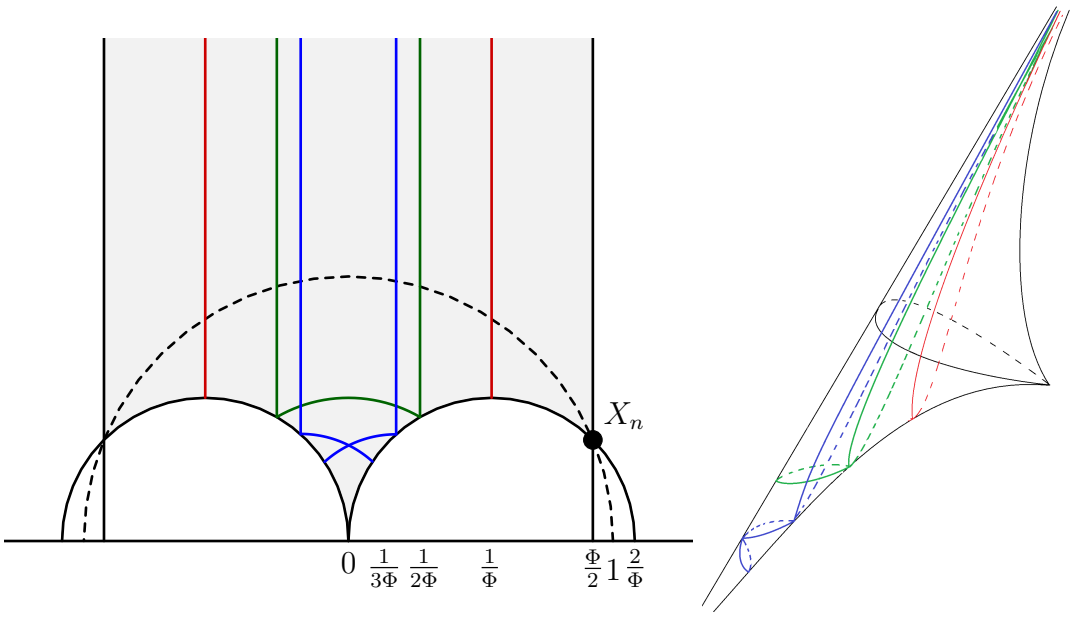

Figure 1: The geodesics $\gamma_{\infty,\frac{1}{k\Phi}}$ for $k = 1, 2, 3$ and their images by the Veech group intersecting the fundamental domain $\mathcal{T}_{nn}$. On the right, the same geodesics on the surface $\mathbb{H}^2/\Gamma_n$.

Specifically when $X = X_n$ is the regular n-gon, the result of Theorem 1.1 can be stated as follows[1]:

Theorem 1.2. *Let $n \geq 8$, $n \equiv 0 \mod 4$. Let l_0 be the length of the side of the n-gon[2]. For any pair of saddle connections α, β, we have*

$$\frac{\mathrm{Int}(\alpha, \beta)}{l(\alpha)l(\beta)} \leq \frac{1}{l_0^2}. \tag{3}$$

Moreover, equality is achieved if and only if α and β are distinct sides of the n-gon.

Using that the volume of a regular n-gon of unit side is $\frac{n}{4\tan\frac{\pi}{n}}$, we get:

Corollary 1.3. *For any $n \geq 8$ such that $n \equiv 0 \mod 4$, we have:*

$$\mathrm{KVol}(X_n) = \frac{n}{4\tan(\frac{\pi}{n})}.$$

[1] Although stated in this order, we first prove Theorem 1.2 and then use it to prove Theorem 1.1

[2] Which is also the systolic length of the resulting surface X_n.

Notice that although X_n has minimal KVol in its Teichmüller disk, it is not a local minimum for KVol in its stratum $\mathcal{H}(2g-2)$. Indeed, the regular n-gon is the polygon with n sides of the same length that have maximal volume. In particular, any other such polygon close to the regular n-gon will have a smaller volume, and KVol will still be realized by pairs of sides of the corresponding n-gon, hence will be smaller.

The case $n \equiv 2 \mod 4$. If $n \equiv 2 \mod 4$, the resulting translation surface X_n has two conical singularities, so that saddle connections may not be closed curves anymore, and simple closed geodesics could be homologous to the union of several non-closed saddle connections in different directions. For this reason, we do not have a closed formula for KVol in the Teichmüller disk of the regular n-gon. However, we show:

Theorem 1.4. *For $n \geq 10$ with $n \equiv 2 \mod 4$, KVol is bounded on the Teichmüller disk of the regular n-gon.*

An explicit bound is given in Corollary 6.3. This result contrasts with examples of squared tiled translation surfaces with multiple singularities having unbounded KVol on their Teichmüller disk. It is the first example of a translation surface with more than one singularity where we can show boundedness on the Teichmüller disk. In fact, we give an explicit boundedness criterion in the Teichmüller disk of a Veech surface:

Theorem 1.5. KVol *is bounded on the Teichmüller disk of a Veech surface X if and only if there are no intersecting closed curves η and ξ on X such that $\eta = \eta_1 \cup \cdots \cup \eta_k$ and $\xi = \xi_1 \cup \cdots \cup \xi_l$ are unions of parallel saddle connections (that is all saddle connections $\eta_1, \ldots, \eta_k, \xi_1, \ldots, \xi_l$ have the same direction).*

This criterion generalises Proposition 3.2 of [BLM22] to the case of translation surfaces with several singularities.

Finally, concerning the regular n-gon itself, the proof of Theorem 1.2 extends and gives:

Theorem 1.6. *Let $n \geq 10$ with $n \equiv 2 \mod 4$. Let l_0 be the length of the side of the n-gon. For any pair of closed curves α, β on X_n, we have*

$$\frac{Int(\alpha, \beta)}{l(\alpha) l(\beta)} < \frac{1}{l_0^2}.$$

Notice that in this case, we show that the inequality is strict. In fact, it is unclear whether the best possible ratio is achieved and, if so, by which closed curves. Our guess would be the following:

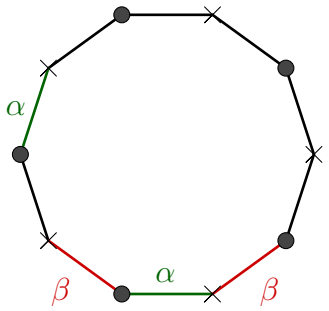

Figure 2: In this example, the curves α and β (oriented such that the resulting curve has a well defined orientation) intersect twice.

Conjecture 1.7. *Let $n \geq 10$ with $n \equiv 2 \mod 4$. For any pair of closed curves α, β on X_n, we have*

$$\frac{Int(\alpha,\beta)}{l(\alpha)l(\beta)} \leq \frac{1}{2l_0^2},$$

where l_0 is the length of the side of the n-gon. Moreover, equality is achieved if and only if α and β are twice intersecting pairs of sides of the n-gon, as in Figure 2 for the decagon. In particular:

$$\mathrm{KVol}(X_n) = \frac{n}{8\tan(\frac{\pi}{n})}$$

Strategy of proof. Although stated in the reversed order, the proof of Theorem 1.1 rely on Theorem 1.2. The proof of both Theorem 1.2 and Theorem 1.6 uses a subdivision method developped in [BLM22] in the case of the double n-gon for odd n, which we extend to the case of the regular n-gons for even n: given two saddle connections, we can estimate simulteneously their lengths and their intersection by subdivising each saddle connection into smaller well-chosen segments.

Then, we prove Theorem 1.1 by studying how the ratio $\frac{\mathrm{Int}(\alpha,\beta)}{l(\alpha)l(\beta)}$ varies as the surface X and the saddle connections α and β moves under the action of a matrix of $SL_2(\mathbb{R})$. The proof of both Theorem 1.1 and Theorem 1.4 uses the fact that there are only two cylinder decompositions up to the action of $SL_2(\mathbb{R})$ on each surface of the Teichmüller disk of the regular n-gon.

Further, although Theorem 1.1 is similar to Theorem 1.1 of [BLM22] stated for the double n-gon when n is odd, the main difference is that the maximum of KVol on the Teichmüller disk of the regular n-gon is achieved along an infinite set of geodesics instead of a single geodesic for the Teichmüller disk of the double regular n-gon. This has to do with the fact that the staircase model associated with the double regular n-gon has a pair of intersecting systoles, giving a big KVol,

while there is only one systole for the staircase model associated with the regular n-gon. In particular, the supremum in the definition of KVol on the staircase model associated with the regular n-gon ($n \geq 8$, $n \equiv 0 \mod 4$) is achieved when α and β are respectively the systole and the second shortest closed curve (which is perpendicular to the systole, see Figure 4), but it is also realised as the limit when k goes to infinity of the ratio $\frac{\mathrm{Int}(\alpha,\beta_k)}{l(\alpha)l(\beta_k)}$, where α is the systole and β_k is a saddle connection winding k times around the smallest vertical cylinder of $\mathcal{S}_n$ (and hence intersecting $k+1$ times α, counting one singular intersection).

Organization of the paper. We recall in Section 2 useful results about translation surfaces and their Veech groups, and we describe the staircase model associated with the regular n-gon. In Section 3, we compute explicitly KVol on the regular n-gon using elementary geometry, showing both Theorem 1.2 and Theorem 1.6. Next, we provide in Section 4 key estimates that allows to understand the function KVol on the Teichmüller disk. Using the knowledge of KVol on the regular n-gon ($n \equiv 0 \mod 4$), we prove Theorem 1.1 in Section 5. Finally, we show the boundedness criterion for KVol on Teichmüller disks (Theorem 1.5) in Section 6 and we apply this criterion to the regular n-gon ($n \equiv 2 \mod 4$) in order to deduce Theorem 1.4.

Ackowledgements. I would like to thank Erwan Lanneau and Daniel Massart for their constant support and for enlightening discussions, as well as helpful comments on preliminary versions of this document.

2 Background

2.1 Translation surfaces and their Veech groups

We start with a quick review of useful notions. We encourage the reader to check out the surveys [Zor06], [Wri16] and [Mas22] for a general introduction to translation surfaces.

A *translation surface* (X, ω) is a real compact genus g surface X with an atlas ω such that all transition functions are translations except on a finite set of singularities Σ, along with a distinguished direction. In fact, it can also be seen as a surface obtained from a finite collection of polygons embedded in $\mathbb{C}$ by gluing pairs of parallel opposite sides by translation. The resulting surface has a flat metric and a finite number of conical singularities. With this description, the moduli space of translation surfaces can be thought of as the space of all translation surfaces up to cut and paste.

The action of $GL_2^+(\mathbb{R})$ on polygons induces an action on the moduli space of translation surfaces. The orbit of a given translation surface is called its *Teichmüller disk* and its stabilizer is called the *Veech group* and is often denoted

$SL(X)$. W.A. Veech showed in [Vee89] that the latter are discrete subgroups of $SL_2(\mathbb{R})$. In particular, the Teichmüller disk of a translation surface can be identified with $\mathbb{H}^2/SL(X)$.

2.2 The regular n-gon and its staircase model

Given $n \geq 4$ even, one can contruct a translation surface by identifying parallel opposite sides of a regular n-gon. If $n \equiv 0 \mod 4$ (and $n \geq 8$), the resulting surface has a single singularity, and in particular, every edge corresponds to a closed curve on the surface. However, if $n \equiv 2 \mod 4$ (and $n \geq 10$), the resulting surface has two singularities, so that sides are no longer closed curves.

As described in [Mon05] and depicted in Figures 3 and 4, the regular n-gon X_n has a staircase shaped model $\mathcal{S}_n$ in its Teichmüller disk.

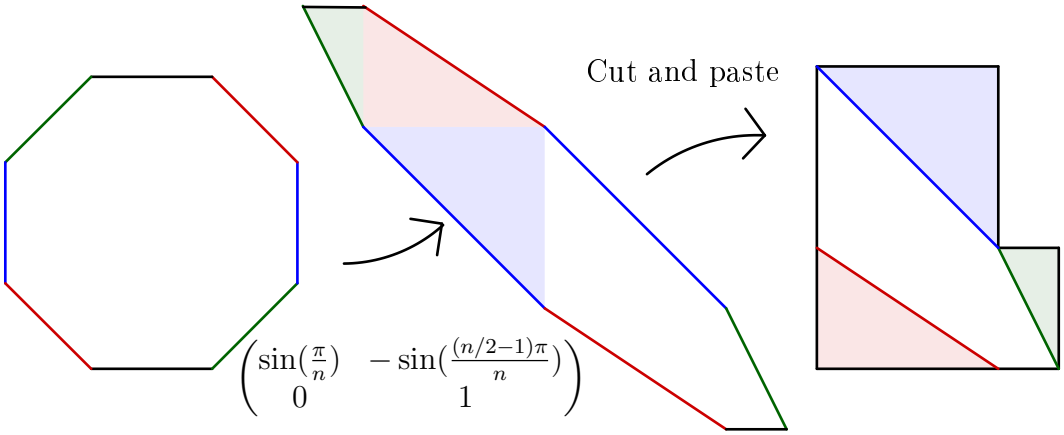

Figure 3: From the regular octagon to its staircase model.

With the notations of Figure 4, the lengths of the sides are given by:

$$l(\alpha_i) = \sin(\frac{(n/2-2i+1)\pi}{n}) \text{ and } l(\beta_j) = \sin(\frac{(n/2-2j+2)\pi}{n})$$

Where $i, j \in [\![1, \frac{n}{4}]\!]$ for $n \equiv 0 \mod 4$, and $i \in [\![1, \frac{n-2}{4}+1]\!]$ while $j \in [\![1, \frac{n-2}{4}]\!]$ for $n \equiv 2 \mod 4$. In particular, the modulus of each vertical cylinder C_i is $\Phi = 2\cos(\frac{\pi}{n})$ as well as the modulus of each horizontal cylinder Z_j, except the horizontal cylinder Z_1 if $n \equiv 0 \mod 4$ (resp. the vertical cylinder C_1 if $n \equiv 2 \mod 4$) having a modulus of $\Phi/2$.

In both cases, the Veech group Γ_n associated with the staircase model contains the horizontal twist $T_H = \begin{pmatrix} 1 & \Phi \\ 0 & 1 \end{pmatrix}$ and the vertical twist $T_V = \begin{pmatrix} 1 & 0 \\ \Phi & 1 \end{pmatrix}$. In fact, it is shown in [Vee89] that Γ_n is generated by T_H and T_V. In particular, the

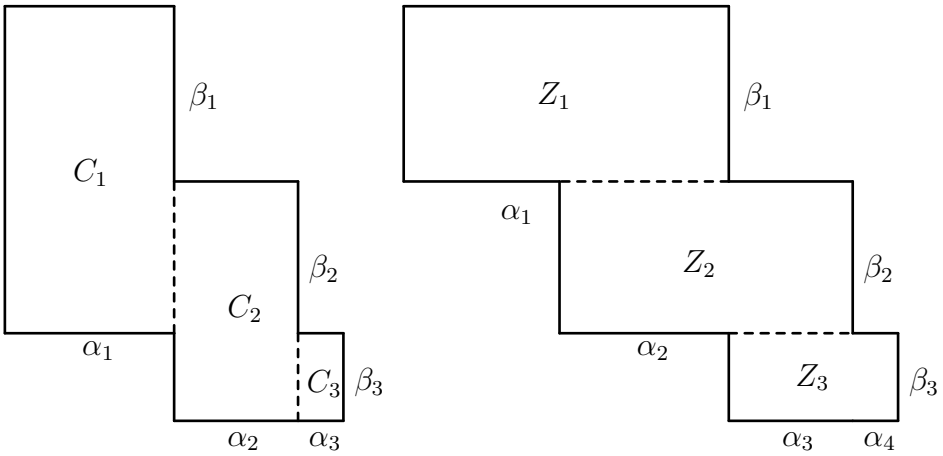

Figure 4: The staircase model associated with the regular n-gon for $n = 12$ on the left and $n = 14$ on the right.

Teichmüller disk of the regular n-gon, identified with $\mathbb{H}^2/\Gamma_n$ has a fundamental domain $\mathcal{T}_n$ as depicted in Figure 5.

It will sometimes be convenient to include orientation-reversing elements in the definition of the Veech group. The matrix $R = \begin{pmatrix} 1 & 0 \\ 0 & -1 \end{pmatrix}$ gives an affine orientation-reversing diffeomorphism of the staircase model, and in fact T_H, T_V and R generate the "non-oriented" Veech group, which we will denote by $\Gamma_n^{\pm}$.

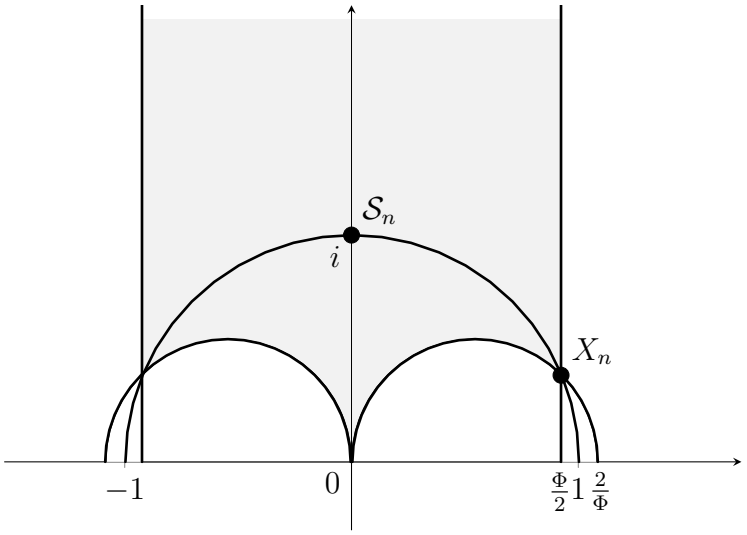

Figure 5: The fundamental domain of the Teichmüller disk of X_n.

3 KVol on the regular n-gon, $n \equiv 0 \mod 4$.

In this section, we give an elementary proof of Theorem 1.2 and Theorem 1.6. The main idea of the proof is to subdivide saddle connections α and β into smaller (non-closed) segments where we can control both the lengths and the intersections.

Given saddle connections α and β, we start by defining a notion of sector for the direction of α (resp. β) which tells how to subdivide the saddle connection α (resp. β) into segments (§§3.1 & 3.2). Then, we study these segments separately and show that they are all longer than the side of the regular n-gon (§3.2). Finally, we study the possible intersection for each pair of segments (§3.3). Setting aside two particular cases that are studied separately, each pair of segments (α_i, β_j) intersect at most once, giving the desired ratio. To conclude the proof, it remains to take into account the possible singular intersections. This can be acomplished by paying closer attention to the intersections and the lengths.

3.1 Sectors and separatrix diagrams

The directions of the diagonals of the regular n-gon subdivide the set of possible directions into n sectors of angle $\frac{\pi}{n}$, as in Figure 6 for the octagon.

In each sector there is an associated *transition diagram* which encodes the possible sequence of intersections of sides for a line whose direction lies in this sector. For example, a geodesic with direction in the sector Σ_0 of Figure 6 has to intersect e_2 before and after each intersection with e_1 while it can intersect either e_2 or e_3 before and after each intersection with e_0. In this example, the sector Σ_0 gives the following transition diagram:

$$e_1 \leftrightarrows e_2 \leftrightarrows e_0 \leftrightarrows e_3 \circlearrowleft$$

In this configuration we say that e_1 is *sandwiched*. The side e_1 can only be preceded and followed by the (adjacent) side e_2. More generally, for a given sector Σ on the regular n-gon we have a separatrix diagram of the form

$$e_{\sigma(0)} \leftrightarrows e_{\sigma(1)} \leftrightarrows \cdots \leftrightarrows e_{\sigma(n/2-2)} \leftrightarrows e_{\sigma(n/2-1)} \circlearrowleft$$

where $\sigma = \sigma_\Sigma \in \mathfrak{S}_{n/2}$ is a given permutation. We say that the side $e_{\sigma(0)}$ is sandwiched by the side $e_{\sigma(1)}$ in sector Σ. Note that it is sufficient to know $\sigma(0)$ and $\sigma(1)$ to tell the sector, as the sector is defined by the directions of the side $e_{\sigma(0)}$ and the diagonal $e_{\sigma(0)} + e_{\sigma(1)}$. See [SU] for further details on transition diagrams of regular n-gons.

3.2 Construction of the subdivision.

Let α be an oriented saddle connections on the regular n-gon. Assume α is not a diagonal of the n-gon, so that it has a well defined sector Σ_α which corresponds

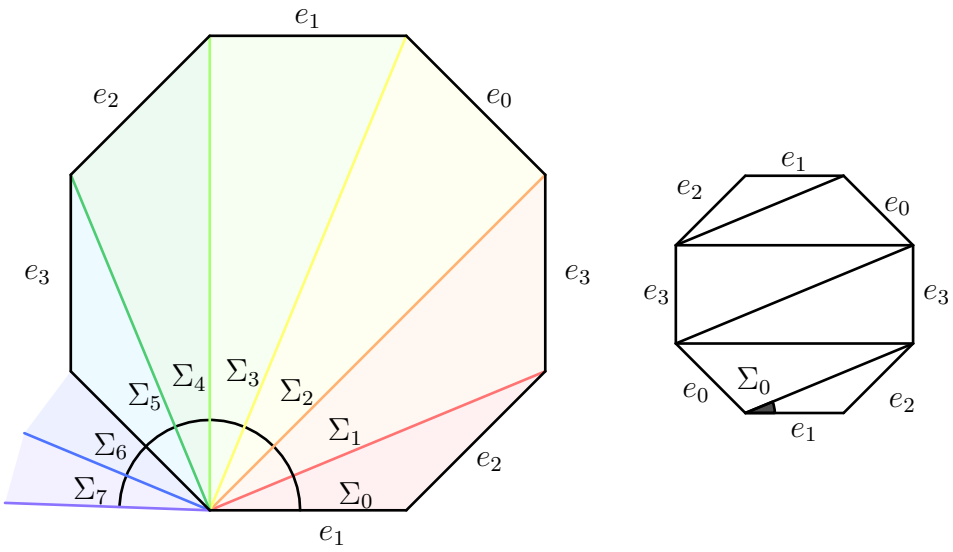

Figure 6: The directions of the diagonals of the octagon divide the set of directions into 8 sectors. On the right, diagonals corresponding to the sector Σ_0.

to a transition diagram given by the permutation σ_α. We cut α each time it intersects a non-sandwiched side of the n-gon. This gives a decomposition into non-closed segments $\alpha = \alpha_1 \cup \cdots \cup \alpha_k$ where each segment is either (see Figure 7):

- A non-sandwiched segment which goes from a side of the n-gon to another non-adjacent side of the n-gon.
- A sandwiched segment, with extremities on the side $e' = e_{\sigma_\alpha(1)}$, intersecting the sandwiched side $e = e_{\sigma_\alpha(0)}$ on its interior. Such segments are made of one piece going from e' to e and another piece going from e to e'. We say that such a sandwiched segment has type $e' \to e \to e'$.
- An initial or terminal segment α_1 or α_k. Such segments will be considered as non-sandwiched segments.

If α is a diagonal or a side of the n-gon, we set $k = 1$ and $\alpha = \alpha_1$.
By construction, we have:

Lemma 3.1. *For every i, we have $l(\alpha_i) \geq l_0$ and equality holds if and only if $k = 1$ and α is a side of the regular n-gon.*

Proof. A non-sandwiched segment has length at least l_0 since each segment going from a side to another non-adjacent side has length at least l_0 in the regular n-gon.
Now, take a sandwiched segment and assume up to a rotation that it is of type $e_2 \to e_1 \to e_2$, as in Figure 7. Since angles between the sides e_1 and e_2 are obtuse, the sandwiched segment has a length bigger than the length of e_1, that is l_0. □

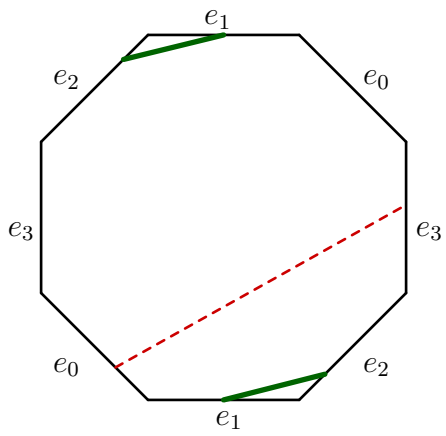

Figure 7: Example of a non-sandwiched segment (in dashed red) and a sandwiched segment (in bold green). The sandwiched segment is of type $e_2 \to e_1 \to e_2$.

3.3 Study of the intersections

In this section, we investigate the possible intersections between two distinct saddle connections α and β, and show:

$$\frac{|\alpha \cap \beta| + 1}{l(\alpha) l(\beta)} \leq \frac{1}{l_0^2} \tag{4}$$

where $|\alpha \cap \beta|$ is the cardinal of the set of intersection points without counting the singularities. This set is finite as α and β are distinct saddle connections.

As before, we decompose both $\alpha = \alpha_1 \cup \cdots \cup \alpha_k$ and $\beta = \beta_1 \cup \cdots \cup \beta_l$ into sandwiched and non-sandwiched segments. We start with the case where either α or β are sides of the n-gon.

If α (resp. β) is a side of the n-gon. In this case, notice that:

1. Between each non-singular intersection with α, there is at least one sandwiched segment or one non-sandwiched segment of β, giving a length greater than l_0.
2. Further, after the last non singular intersection with α, there is a least one non-sandwiched segment, giving a length greater than l_0.
3. If there are no non-singular intersection with α, then β has length at least l_0 anyway (with equality if and only if β is another side of the regular n-gon).

In particular, $l(\beta) \geq (|\alpha \cap \beta| + 1) l_0$ and hence:

$$\frac{|\alpha \cap \beta| + 1}{l(\alpha) l(\beta)} \leq \frac{1}{l_0^2}$$

with equality if and only if both α and β are sides of the regular n-gon.

The other cases. In the rest of this section, we assume that α and β are not both sides of the regular n-gon. As such, there is at least one segment α_i of α for which the inequaltity $l(\alpha_i) > l_0$ is strict, and hence $l(\alpha)l(\beta) > kl \cdot l_0^2$. Further, up to a small deformation of α, we can assume there are no intersection on the sides of the n-gon (it is possible to do it while keeping each α_i straight and in the same sector). In this setting, all non-singular intersections between α and β correspond to an intersection of two segments α_i and β_j and we have:

$$|\alpha \cap \beta| \leq \sum_{i,j} |\alpha_i \cap \beta_j|$$

where $|\alpha_i \cap \beta_j|$ is the number of intersection points between the (non-closed) curves α_i and β_j. The latter quantity is finite as long as α and β are assumed to be distinct. Notice that if $n \equiv 0 \mod 4$, there is a single singularity so that α and β are automatically closed curves and we can define their algebraic intersection, and hence:

$$\mathrm{Int}(\alpha, \beta) \leq (\sum_{i,j} |\alpha_i \cap \beta_j|) + 1 \tag{5}$$

where the added $+1$ corresponds to the possible singular intersection.

Now, remark that if both α_i and β_j are not sandwiched, then $|\alpha_i \cap \beta_j| \leq 1$. More generally, we have:

Lemma 3.2. *For any i, j, $|\alpha_i \cap \beta_j| \leq 2$. Further, the case $|\alpha_i \cap \beta_j| = 2$ is possible only if:*

(i) Either α_i is a sandwiched segment of type $e' \to e \to e'$ and β_j is a sandwiched segment of type $e \to e' \to e$.

(ii) Or, up to permutation of α and β, α_i is a sandwiched segment of type $e' \to e \to e'$, and β_j is a long segment, that is the endpoints of β_j lie in $e_{\sigma_\beta(2m-1)}$ or $e_{\sigma_\beta(2m-2)}$ or at the two vertices contained in both $e_{\sigma_\beta(n/2-1)}$ and $e_{\sigma_\beta(n/2-2)}$. Further, $\{e, e'\} = \{e_{\sigma_\beta(n/2-1)}, e_{\sigma_\beta(n/2-2)}\}$.

These two configurations are depicted in Figure 8.

Remark 3.3. Notice that the two cases cannot happen simultaneously since in case (i) we have $\{e, e'\} = \{e_{\sigma_\beta(1)}, e_{\sigma_\beta(0)}\}$ while in case (ii) we have $\{e, e'\} = \{e_{\sigma_\beta(n/2-1)}, e_{\sigma_\beta(n/2-2)}\}$.

Proof of Lemma 3.2. 1^{st} **case:** Assume that both α_i and β_j are sandwiched segments. Then, the study of the intersections is exactly the same as the study of the intersections of pairs of sandwiched segments in the double n-gon for odd n, see [BLM22, §6.3]. Up to a rotation or a symmetry, we can assume α_i is sandwiched

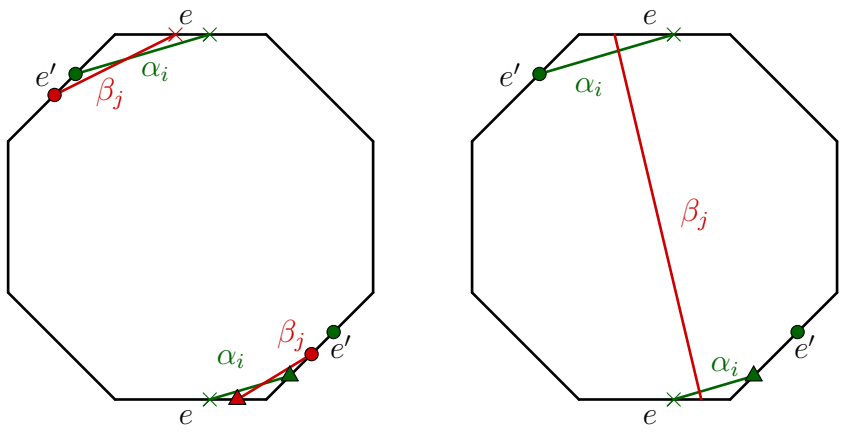

Figure 8: The two cases where $|\alpha_i \cap \beta_j| = 2$.

of type $e_2 \to e_1 \to e_2$.

In particular, $|\alpha_i \cap \beta_j| = 0$ unless β_j has one of the following type:

(1)	$e_0 \to e_1 \to e_0$	(2)	$e_1 \to e_0 \to e_1$
(3)	$e_1 \to e_2 \to e_1$	(4)	$e_2 \to e_1 \to e_2$
(5)	$e_2 \to e_3 \to e_2$	(6)	$e_3 \to e_2 \to e_3$

(This is because α_i and β_j have to share at least a common side of the n-gon to intersect).

Similarly to the case of the double n-gon for odd n, we can show (see Figure 9) that in all cases but (3) we have $|\alpha_i \cap \beta_j| \leq 1$. In particular, the case (3) is the only case where we possibly have $|\alpha_i \cap \beta_j| = 2$ (as in the left of Figure 8).
2^{nd} **case:** Up to permutation of α and β, α_i is sandwiched (say of type $e' \to e \to e'$) while β_j is not. In this case, we see easily that β_j has to be a long segment whose extremities lie on the sides e or e' in order to get two intersections, as in the right of Figure 8. □

In light of Lemma 3.2 and Remark 3.3, we distinguish three mutually exclusive cases:

(0) There is no configuration of type (i) or (ii).

(i) There exists i, j such that α_i and β_j are in a configuration of type (i).

(ii) There exists i, j such that α_i and β_j are in a configuration of type (ii).

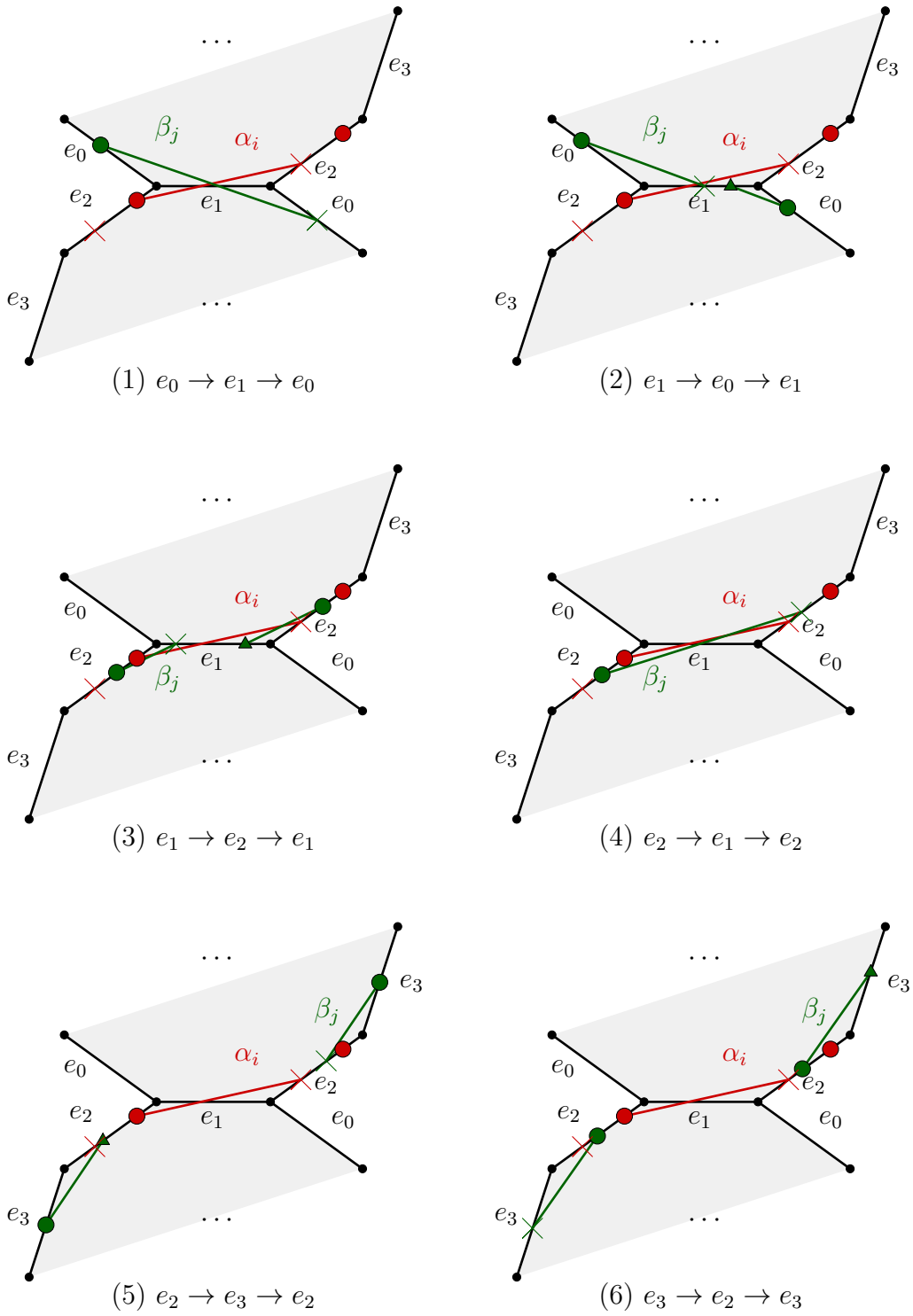

Figure 9: The six cases in Lemma 3.2, (i).

Case (0): There is no configuration of type (i) or (ii). In this case, we deduce from Equation (5) and Lemma 3.2 that:

$$|\alpha \cap \beta| \leq kl. \tag{6}$$

In order to get Equation (4), we either improve the inequality on the intersections (Equation (6)) or the inequality on the lengths $l(\alpha)l(\beta) > kl \cdot l_0^2$. For this purpose, we distinguish two cases:

1. If α is not contained in the cylinder defined by $e_{\sigma_\alpha(0)}, e_{\sigma_\alpha(1)}$ as in Figure 10 (in the example of the octagon), then we can find two consecutive segments α_i and α_{i+1} which are not contained in the cylinder. As explained in Figure 10, the length $l(\alpha_i)+l(\alpha_{i+1})$ should be at least $\Phi^2 l_0$. Since $\Phi^2 > 3$, we have $l(\alpha_i) + l(\alpha_{i+1}) > 3l_0$, so that $l(\alpha) > (k+1)l_0$, and

   $$l(\alpha)l(\beta) > (kl+1)l_0^2.$$

   Using Equation (6) we have directly that Equation (4) holds (the inequality being strict in this case). By symmetry, the same argument holds if β is not contained in the cylinder defined by $e_{\sigma_\beta(0)}, e_{\sigma_\beta(1)}$.

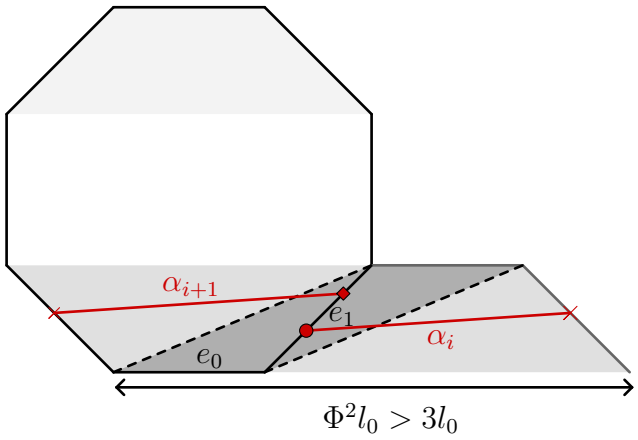

Figure 10: If α is not contained in the cylinder defined by e_0 and e_1, then there are two consecutive segments α_i and α_{i+1} with $l(\alpha_i) + l(\alpha_{i+1}) > 3l_0$.

2. Otherwise, we can assume that α is contained in the cylinder defined by $e_{\sigma_\alpha(0)}$ and $e_{\sigma_\alpha(1)}$ while β is contained in the cylinder defined by $e_{\sigma_\beta(0)}$ and $e_{\sigma_\beta(1)}$. In this case, unless β is a diagonal, we see that α_1 cannot intersect both β_1 (which lies in a region S_0 as in Figure 11) and β_l (which lie in a symmetric region S_1), so that

   $$|\alpha \cap \beta| \leq kl - 1.$$

In particular $|\alpha \cap \beta| + 1 \leq kl$ and using that $l(\alpha)l(\beta) > kl \cdot l_0^2$, we deduce that Equation (4) holds (and the inequality is strict in this case).

3. Finally, if both α and β are diagonals, we have $l(\alpha), l(\beta) \geq \Phi l_0$ and hence $l(\alpha)l(\beta) \geq \Phi^2 l_0^2 > 2l_0^2$, so that Equation (4) holds as well and the inequality is strict.

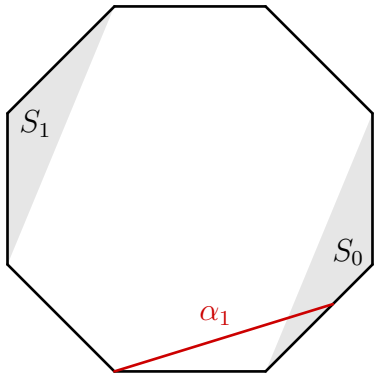

Figure 11: In case 2, α_1 cannot intersect both β_1 (which lies in a region S_0) and β_l (which lies in the symetric region S_1). In this example β has direction in Σ_2.

It remains to investigate cases (i) and (ii).

Case (i): $\exists i, j$, α_i and β_j are in a configuration of type (i), that is α_i is a sandwiched segment of type $e' \to e \to e'$ and β_j is a sandwiched segment of type $e \to e' \to e$. This case corresponds to case (3) of [BLM22, §6.3]. Similarly, we consider the maximal sequence of sandwiched segments $\alpha_{i_0} \cup \cdots \cup \alpha_{i_0+p}$ (resp. $\beta_{j_0} \cup \cdots \cup \beta_{j_0+q}$) containing α_i (resp. β_j), which is maximal in the sense that both α_{i_0-1} and α_{i_0+p+1} (resp. β_{j_0-1} and β_{j_0+q+1}) are non-sandwiched, and we can show:

Lemma 3.4. *$\alpha_{i_0} \cup \cdots \cup \alpha_{i_0+p} \cup \alpha_{i_0+p+1}$ and $\beta_{j_0} \cup \cdots \cup \beta_{j_0+q} \cup \beta_{j_0+q+1}$ intersect at most $(p+3)(q+2)$ times while there are $(p+3)(q+3)$ pairs of segments.*

In particular, summing the intersections of pairs of maximal sequences of sandwiched segments and intersections of pairs of segments which are not already counted in such maximal sequences (and as such intersect at most once), we get:

$$\sum_{i,j} |\alpha_i \cap \beta_j| < kl$$

so that $|\alpha \cap \beta| + 1 \leq kl$ and $\dfrac{|\alpha \cap \beta| + 1}{l(\alpha)l(\beta)} < \dfrac{1}{l_0^2}$, as required.

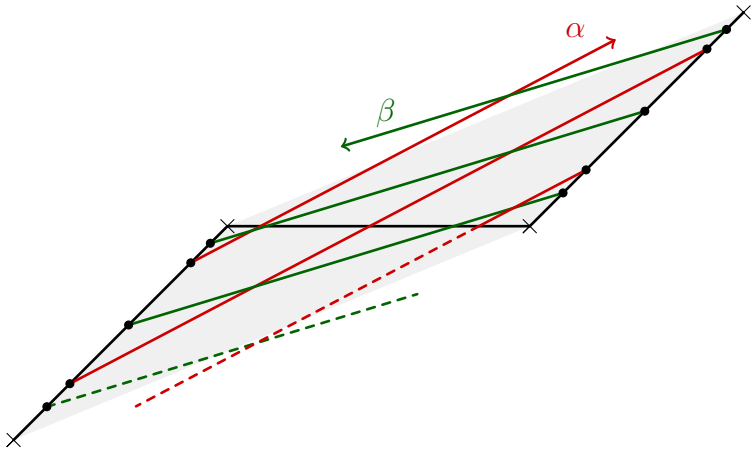

Figure 12: Exemple of maximal sequences of sandwiched segments. In this example, $p = 1$ and $q = 1$. There are 5 intersections.

Case (ii)**:** $\exists i, j$**,** α_i **and** β_j **are in a configuration of type** (ii)**.** In this case, we count the intersection of α with the maximal sequence of non-adjacent segments β_j contained in the big cylinder spanned by $e_{\sigma_\beta(n/2-1)}$ and $e_{\sigma_\beta(n/2-2)}$. Examples are depicted in Figure 13 and Figure 14 in the case of the octagon.

We distinguish two cases: one where we can get a better estimation of the length of β while in the other we can get a better lower bound on the number of intersections between α and β.

1. If β contains only non-sandwiched segments contained in the big cylinder, then in particular β start and end at the vertices which are the common endpoints to the sides of label $e_{\sigma_\beta(n/2-1)}$ and $e_{\sigma_\beta(n/2-2)}$, see Figure 13). In this case, $\beta = \beta_1 \cup \cdots \cup \beta_l$ could have $l + 1$ intersections with α_i (instead of l). However, we can compensate with a better estimation of the lengths. A convenient way to estimate the length is to unfold the big cylinder as in Figure 13 and get:

   - If l is odd, then $l(\beta) \geq (\frac{l+1}{2}\Phi^2 - 1)l_0$.
   - If l is even, then $l(\beta) \geq \frac{l}{2}\Phi^2 l_0$.

   Hence, in both cases, we have $\dfrac{|\alpha_i \cap \beta|}{l(\alpha_i)l(\beta)} < \dfrac{1}{l_0^2}$. Further, the same holds if α_i is a non-sandwiched segment: in this case α_i intersect β at most l times, so that $\dfrac{|\alpha_i \cap \beta| + 1}{l(\alpha_i)l(\beta)} < \dfrac{1}{l_0^2}$. Since α_1 is non-sandwiched, this allows to count the singular intersection, so that:

$$\frac{(\sum_i |\alpha_i \cap \beta|) + 1}{(\sum_i l(\alpha_i))l(\beta)} < \frac{1}{l_0^2}.$$

As required.

2. Else, the maximal sequence $B = \beta_{j_0} \cup \cdots \cup \beta_{j_0+p-1}$ of non-sandwiched segments in the big cylinder containing β_j is not contained big cylinder, as in Figure 14. In this case, given that p is the number of non-sandwiched segments in the maximal sequence, there are at most

   - p intersections, if β either start or end at the central singularity. That is we can assume up to changing the orientation of β that the maximal sequence of non-sandwiched segments containing β_j is $\beta_1 \cup \cdots \cup \beta_p$, and hence we have
   $$\frac{|\alpha_i \cap B|}{l(\alpha_i)l(B)} < \frac{p}{pl_0^2} = \frac{1}{l_0^2}.$$
   Further, using that in this case, $l(\beta_1) \geq (\Phi^2 - 1)l_0 > 2l_0$, we deduce that in fact $l(B) = l(\beta_1) + \cdots + l(\beta_p) > 2l_0 + (p-1)l_0 = (p+1)l_0$, so that
   $$\frac{|\alpha_i \cap B| + 1}{l(\alpha_1)l(B)} < \frac{p+1}{(p+1)l_0^2} = \frac{1}{l_0^2}.$$
   Summing all intersections of this kind with the other intersections, we finally get $\dfrac{\mathrm{Int}(\alpha,\beta)}{l(\alpha)l(\beta)} < \dfrac{1}{l_0^2}$ as required.
   - $(p-1)$ intersections, if β does not start and does not end at the central singularity, so that
   $$\frac{|\alpha_i \cap B| + 1}{l(\alpha_i)l(B)} < \frac{(p-1)+1}{pl_0^2} = \frac{1}{l_0^2}.$$
   Similarly, we conclude that $\dfrac{\mathrm{Int}(\alpha,\beta)}{l(\alpha)l(\beta)} < \dfrac{1}{l_0^2}$ as required.

3.4 Conclusion

As shown in the previous section, for any two distinct saddle connections α and β, we have

$$\frac{|\alpha \cap \beta| + 1}{l(\alpha)l(\beta)} \leq \frac{1}{l_0^2} \tag{4}$$

and equality occurs if and only if α and β are sides of the regular n-gon.

Now, any closed curve η (resp. ξ) on the regular n-gon is homologous to a union of saddle connections $\eta = \eta_1 \cup \cdots \cup \eta_k$ (resp. $\xi = \xi_1 \cup \cdots \cup \xi_l$). In this case, we have

$$\mathrm{Int}(\eta, \xi) \leq (\sum_{i,j} |\eta_i \cap \xi_j|) + s$$

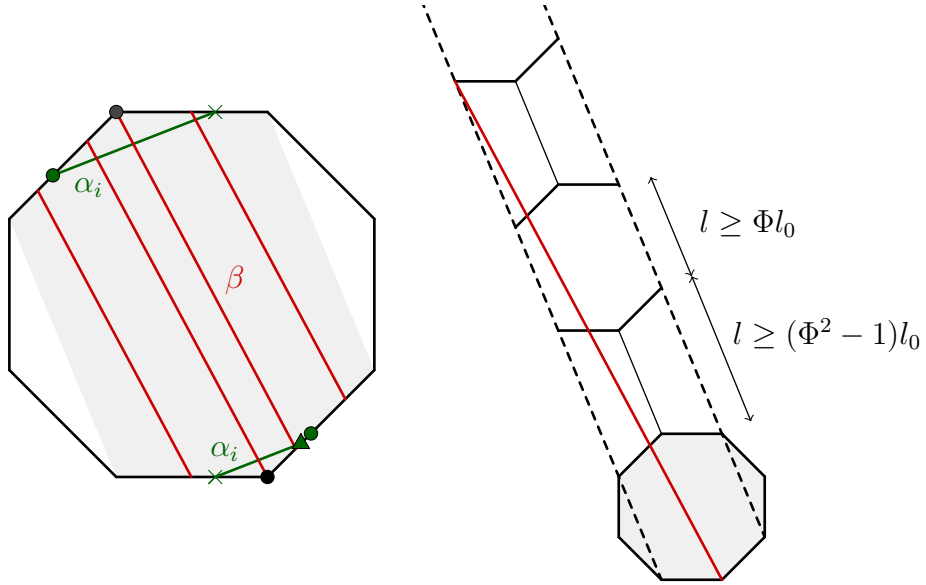

Figure 13: In the case where the curve β stays in the big cylinder, there could be one intersection more (here 5) than non sandwiched segments in β (here 4). However, unfolding the trajectory of the curve β allows to estimate precisely its length, given the lengths of the long diagonals which can be expressed using Φ.

where s is the number singular intersection points. It should be noted that we set $|\eta_i \cap \xi_j| = 0$ if $\eta_i = \xi_j$. Further, we can assume without loss of generality that η and ξ are simple closed curves (see Lemma 3.1 of [MM14]) so that there are no multiple intersections at the singularities, and hence $s \leq \min(k, l)$. Further, $s \leq 1$ for $n \equiv 0 \mod 4$ and $s \leq 2$ for $n \equiv 2 \mod 4$. Using Equation (4), we get:

$$\mathrm{Int}(\eta, \xi) \leq (\sum_{i,j} l(\eta_i) l(\xi_j)) \times \frac{1}{l_0^2} + s - kl = \frac{l(\eta) l(\xi)}{l_0^2} + s - kl$$

with equality if and only if each η_i (resp. ξ_j) is a side of the regular n-gon. In particular:

- For $n \equiv 0 \mod 4$, $s \leq 1$ and we get directly Theorem 1.2, by noticing that distinct sides of the n-gon are indeed intersecting once at the singularity.
- For $n \equiv 2 \mod 4$, if $s \leq 1$ then at least one of the η_i (or ξ_j) is not a side of the n-gon so that $l(\eta_i) > l_0$ (or $l(\xi_j) > l_0$) and

  $$\mathrm{Int}(\eta, \xi) < \frac{l(\eta) l(\xi)}{l_0^2}$$

  Else, if $s = 2$ then $k, l \geq 2$ so that $kl \geq 4$ and

  $$\mathrm{Int}(\eta, \xi) \leq \frac{l(\eta) l(\xi)}{l_0^2} - 2 < \frac{l(\eta) l(\xi)}{l_0^2}$$

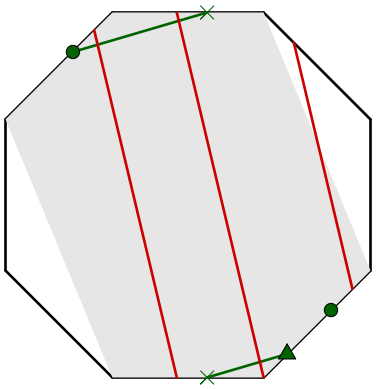

Figure 14: In the case where the curve β leaves the big cylinder, there are at most as many non-sandwiched segments as intersections with the segment α_i.

This gives Theorem 1.6.

4 KVol as a supremum over pairs of directions

In this section, we extend the study of KVol as a function over the Teichmüller disk. We assume $n \equiv 0 \mod 4$ so that X_n has a single singularity (as well as all the translation surfaces in its Teichmüller disk). The study follows the method of [BLM22], but the case of the regular n-gon requires more precise estimates.

We first give a consistent name for saddle connections as the surface varies in the Teichmüller disk, as well as the direction of such saddle connections. This is done in §4.1 by choosing a base surface in the Teichmüller disk, namely $\mathcal{S}_n$, the staircase model. Next, for each pair of distinct periodic directions we define a quantity $K(d, d')$ which can be computed on the base surface $\mathcal{S}_n$, and allows for a more convenient expression of KVol (see Proposition 4.4). Finally, we provide in Proposition 4.7 precise estimates on $K(d, d')$. These estimates are one of the main ingredients in the proof of Theorem 1.1, and they differ from the case of the double n-gon.

4.1 Directions in the Teichmüller disk

Following [BLM22, §4], we consider the plane template of $\mathcal{S}_n$ as our base surface and define the direction of a saddle connection α in $X = M \cdot \mathcal{S}_n$ as the direction (in $\mathbb{R}P^1$) of the preimage saddle connection $M^{-1} \cdot \alpha$ in $\mathcal{S}_n$ it corresponds to. More precisely:

Definition 4.1. For $d \in \mathbb{R}P^1$, we say that a saddle connection in $\mathcal{S}_n$ has direction d if it has direction d in the plane template of Figure 15. For $M \in \mathrm{GL}_2^+(\mathbb{R})$ we

say that a saddle connection α in $M \cdot \mathcal{S}_n$ has direction d if $M^{-1} \cdot \alpha$ has direction d in $\mathcal{S}_n$.

This is a bit counter-intuitive because α may not have direction d in a plane template for $M \cdot \mathcal{S}_n$, but it allows for a consistent choice of the notion of direction along the Teichmüller space. Moreover, we have:

Proposition 4.2. *[BLM22, §4] Using the identifications*

$$d = [x : y] \in \mathbb{R}P^1 \mapsto -\frac{x}{y} \in \mathbb{R} \cup \{\infty\} \equiv \partial\mathbb{H}^2$$

and for $M = \begin{pmatrix} a & b \\ c & d \end{pmatrix} \in SL_2(\mathbb{R})$

$$M \cdot \mathcal{S}_n \in \mathcal{T}_n \mapsto \frac{di + b}{ci + a} \in \mathbb{H}^2,$$

the locus of surfaces in $\mathcal{T}_n$ *where the directions* d *and* d' *make an (unoriented) angle* $\theta \in]0, \frac{\pi}{2}]$ *is the banana neighborood*

$$\gamma_{d,d',r} = \{z \in \mathbb{H}^2 : \mathrm{dist}_{\mathbb{H}^2}(z, \gamma_{d,d'}) = r\}$$

where $\cosh r = \dfrac{1}{\sin\theta}$.

In particular, the locus of surfaces in $\mathcal{T}_n$ *where the directions* d *and* d' *are orthogonal is the hyperbolic geodesic with endpoints* d *and* d'.

In the rest of the paper, we use the following

Notation 4.3. Given $X = M \cdot \mathcal{S}_n \in \mathcal{T}_n$, and d, d' distinct periodic directions, we define $\theta(X, d, d') \in]0, \frac{\pi}{2}]$ as the (unoriented) angle between the directions d and d' in the surface X. With this notation, we have by Proposition 4.2:

$$\sin\theta(X, d, d') = \frac{1}{\cosh(\mathrm{dist}_{\mathbb{H}^2}(X, \gamma_{d,d'}))}. \tag{7}$$

4.2 KVol as a supremum over pairs of directions

With the above choice of a consistent name for saddle connections and directions along the Teichmüller disk, we have the following proposition, which is already stated in [BLM22] in the case of the double n-gon but can be extended with the same proof to the case of translation surfaces S for which saddle connections in the same direction do not intersect.

Proposition 4.4. *[BLM22, Proposition 5.1] Let S be a translation surface with a single singularity such that saddle connections in the same direction are non-intersecting. Let $\mathcal{P}$ be the set of directions of saddle connections of S. Define the notion of direction for X in the Teichmüller disk of S using Definition 4.1. Then, for any surface X in the Teichmüller disk of S, we have:*

$$\mathrm{KVol}(X) = \mathrm{Vol}(X) \cdot \sup_{\substack{d, d' \in \mathcal{P} \\ d \neq d'}} K(d, d') \cdot \sin\theta(X, d, d'), \tag{8}$$

where $K(d, d') = \sup_{\substack{\alpha \subset \mathcal{S}_n \text{ saddle connection in direction } d \\ \beta \subset \mathcal{S}_n \text{ saddle connection in direction } d'}} \frac{\mathrm{Int}(\alpha,\beta)}{\alpha \wedge \beta}$ and $\theta(X, d, d')$ is the angle given by Notation 4.3.

The fact that saddle connections in the same direction on the regular n-gon are non-intersecting can be checked using the horizontal and vertical cylinder decomposition of the staircase model.

Remark 4.5. Notice that the Veech group $\Gamma_n^{\pm}$ of the staircase model $\mathcal{S}_n$ acts on $\mathcal{S}_n$ while preserving the intersection form, and acts linearly on $\mathbb{R}^2$, hence preserving the wedge product. In particular, $K(d, d') = K(g \cdot d, g \cdot d')$ for any element $g \in \Gamma_n^{\pm}$.

From this result and Theorem 1.2, we deduce

Corollary 4.6. *For $n \geq 8, n \equiv 0 \mod 4$, we have:*

$$\mathrm{KVol}(X_n) = \mathrm{Vol}(X) \cdot K(\infty, \frac{1}{\Phi}) \cdot \sin\theta(X_n, \infty, \frac{1}{\Phi})$$

In particular,

$$\forall (d, d'),\ K(d, d') \cdot \sin\theta(X_n, d, d') \leq K(\infty, \frac{1}{\Phi}) \cdot \sin\theta(X_n, \infty, \frac{1}{\Phi}).$$

Proof. By Theorem 1.2, KVol is achieved on the regular n-gon by pairs of distinct sides. In particular, the sides of the n-gon α and β corresponding to directions ∞ and $\frac{1}{\Phi}$ achieve the supremum:

$$\begin{aligned}
\mathrm{KVol}(X_n) &= \frac{\mathrm{Int}(\alpha, \beta)}{l(\alpha) l(\beta)} \text{ by Theorem 1.2.} \\
&= \frac{\mathrm{Int}(\alpha, \beta)}{\alpha \wedge \beta} \sin angle(\alpha, \beta) \\
&= K(\infty, \frac{1}{\Phi}) \sin\theta(X_n, \infty, \frac{1}{\Phi}) \text{ by definition of } K(d, d') \text{ and } \theta(X, d, d').
\end{aligned}$$

□

Next, we provide precise estimates on $K(d, d')$ using its invariance under the diagonal action of the Veech group. These estimates are one of the main ingredients in the proof of Theorem 1.1.

Proposition 4.7. *For any pair of distinct periodic directions (d, d'), we have, with the notations of Figure 15:*

- ♠ *If there exist $k \in \mathbb{N}^* \cup \{\infty\}$ and $g \in \Gamma_n^{\pm}$ such that $(d, d') = (g \cdot \infty, \pm g \cdot \frac{1}{k\Phi})$, we have*
$$K(d, d') = \frac{1}{l(\alpha_1)l(\alpha_m)} = \frac{1}{\Phi l_m^2}$$
with $l_m := l(\alpha_m)$.

- ♦ *If there exist $g \in \Gamma_n^{\pm}$ such that $(d, d') = (g \cdot \infty, \pm g \cdot \frac{\Phi^2-1}{\Phi^3-2\Phi})$, then*
$$K(d, d') = \frac{1}{(\Phi^3 - 2\Phi)l_m^2} = \frac{1}{\Phi^2 - 2} K(\infty, \frac{1}{\Phi}).$$
This is the case of $(d, d') = (\frac{1}{\Phi}, \Phi - \frac{1}{\Phi})$, image of $(\infty, \frac{\Phi^2-1}{\Phi^3-2\Phi})$ by the element $g = T_V R \in \Gamma^{\pm}$.

- *In the other cases,*
$$K(d, d') < \frac{1}{(\Phi^3 - 2\Phi)l_m^2}.$$

Recall that the α_i (resp. β_j) are the horizontal (resp. vertical) saddle connection sorted by decreasing length, and define $l_i := l(\alpha_i)$ and $h_j := l(\beta_j)$ for $1 \leq i, j \leq m$. Further, we denote $C_1, \ldots, C_m$ (resp. $Z_1, \ldots, Z_m$) the vertical (resp. horizontal) cylinders, as in Figure 15. Using that the moduli of both horizontal and vertical cylinders are all $1/\Phi$ (except the horizontal cylinder Z_1), one can compare the lengths h_m, h_{m-1} and l_{m-1} to l_m, as in Figure 16.

Proof. The proof goes as follow: given a pair of distinct periodic directions (d, d') and a pair of saddle connections (α, β) in respective directions d, d', we first notice that it is possible to assume that α is either horizontal ($d = \infty$, i.e $\alpha = \alpha_i$ for $i \in [\![1, m]\!]$) or vertical ($d = 0$, i.e $\alpha = \beta_j$ for $j \in [\![1, m]\!]$). This is because $K(d, d')$ is by invariant under the action of the Veech group and any periodic direction is either the image of the horizontal or the vertical by an element of the Veech group. We study the cases $d = \infty$ and $d = 0$ separately, identify the configurations ♠ and ♦ and show that $K(d, d')$ is smaller in the other cases.

Case 1: d represents the horizontal cusp. Up to the action by an element of the Veech group, we can assume α is one of the α_i. Let us first study the intersection with α_i for $i < m$.

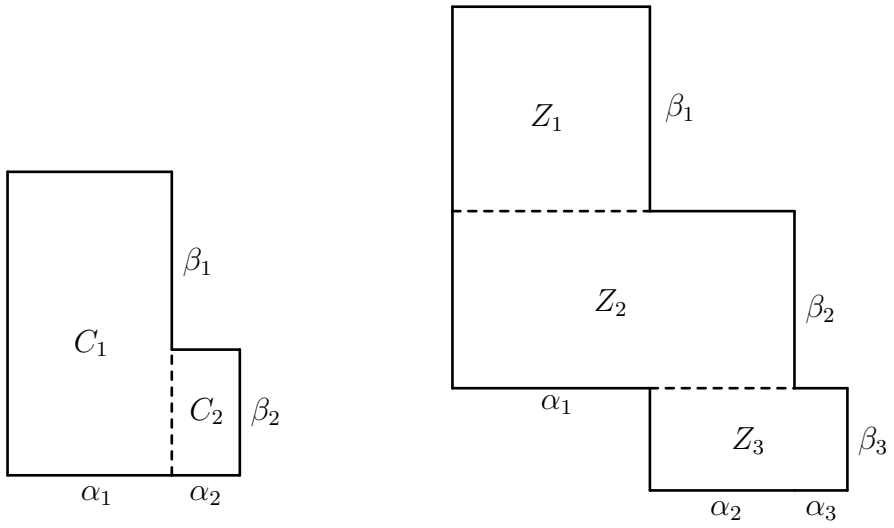

Figure 15: The staircase models associated to the n-gon for $n = 8$ on the left and $n = 12$ on the right, and the cylinders.

Case 1.1: $\alpha = \alpha_i$ for $i < m$.

Lemma 4.8. *For any $i < m$, and any saddle connection β, we have*

$$\frac{\mathrm{Int}(\alpha_i, \beta)}{\alpha_i \wedge \beta} < \frac{1}{\Phi^3 - 2\Phi} \cdot \frac{1}{l_m^2}.$$

Proof. First notice that if a saddle connection β does not intersect the core curves of the cylinders $Z_1, \ldots, Z_m$, we have $\mathrm{Int}(\alpha_i, \beta) = 0$ since the core curves are respectively homologous to $\alpha_1, \alpha_1 + \alpha_2, \cdots, \alpha_{i-1} + \alpha_i$. In particular, a saddle connection β having non-zero intersection with α has a vertical length at least h_i. Further, any non singular intersection of β with α_i for $i < m$ requires a vertical length at least $h_i + h_{i+1}$ (see Figure 17). This gives:

$$\alpha_i \wedge \beta \geq l_i \max((h_i + h_{i+1})(\mathrm{Int}(\alpha_i, \beta) - 1), h_i)$$

In particular,

(i) If $\mathrm{Int}(\alpha_i, \beta) \leq 1$, we use $\alpha_i \wedge \beta \geq l_i h_i$ to get

$$\frac{\mathrm{Int}(\alpha_i, \beta)}{\alpha_i \wedge \beta} \leq \frac{1}{l_i h_i},$$

and, since $i < m$, we get

$$\frac{1}{l_i h_i} \leq \frac{1}{l_{m-1} h_{m-1}} \leq \frac{1}{(\Phi^2 - 1)(\Phi^3 - 2\Phi) l_m^2} < \frac{1}{(\Phi^3 - 2\Phi) l_m^2}.$$

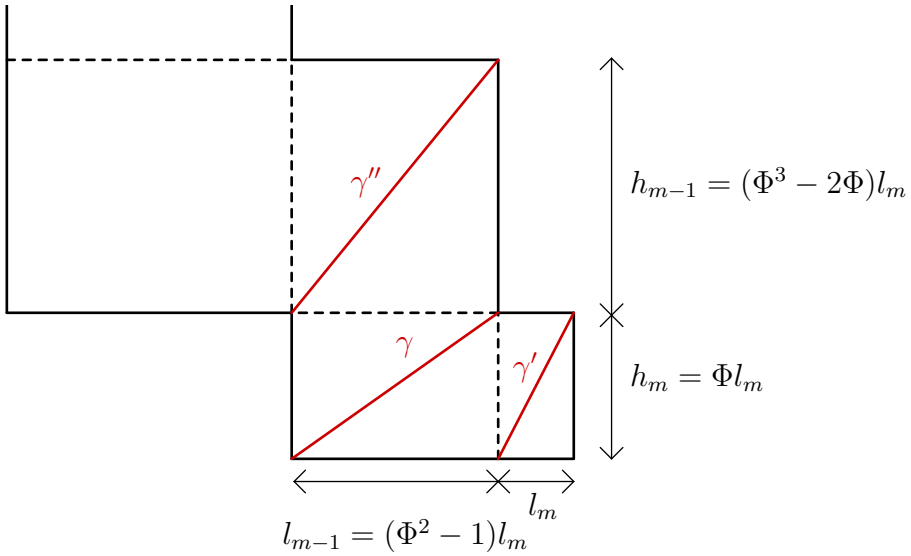

Figure 16: The lengths h_m, h_{m-1} and l_{m-1} expressed using l_m. The diagonal curves γ, γ' and γ'' have respective co-slope $\Phi - \frac{1}{\Phi}$, $\frac{1}{\Phi}$, and $\frac{\Phi^2-1}{\Phi^3-2\Phi}$.

(ii) Otherwise, we use $\alpha_i \wedge \beta \geq l_i(h_i + h_{i+1})(\mathrm{Int}(\alpha_i, \beta) - 1)$ and obtain

$$\frac{\mathrm{Int}(\alpha_i, \beta)}{\alpha_i \wedge \beta} \leq \frac{2}{l_i(h_i + h_{i+1})}.$$

But, since $i < m$, we have $l_i \geq l_{m-1} = (\Phi^2 - 1)l_m$ and $h_i + h_{i+1} \geq h_{m-1} + h_m = (\Phi^3 - \Phi)l_m$ and in particular

$$\frac{2}{l_i(h_i + h_{i+1})} \leq \frac{2}{(\Phi^3 - \Phi)(\Phi^2 - 1)l_m^2} < \frac{1}{(\Phi^3 - 2\Phi)l_m^2},$$

where the last inequality comes from $\Phi^3 - \Phi > \Phi^3 - 2\Phi$ and $\Phi^2 - 1 > 2$.

□

Case 1.2: $\alpha = \alpha_m$. In this case, notice that either β is contained in the horizontal cylinder Z_m (see Figure 15) and, up to a horizontal twist, its co-slope is $\pm\frac{1}{k\Phi}$ for $k \in \mathbb{N}^* \cup \{\infty\}$ so that it corresponds to a geodesic of case ♠, or β is not contained in Z_m.

Case 1.2.i. If the direction of β is, up to an horizontal twist, $d' = \pm\frac{1}{k\Phi}$ as in ♠, and β is contained in Z_m, we see that α and β intersect $k+1$ times and $\alpha \wedge \beta = (k+1)l(\beta_m)l(\alpha_m) = (k+1)\Phi l_m^2$ (see Figure 18 for the case $k = 3$). This gives directly that

$$\frac{\mathrm{Int}(\alpha_m, \beta)}{l(\alpha)l(\beta)} = \frac{k+1}{(k+1)\Phi l_m^2} = \frac{1}{\Phi l_m^2}.$$

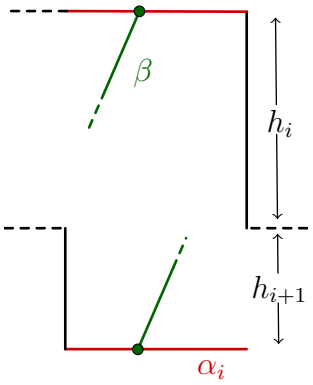

Figure 17: A non singular intersection with α_i, $i < m$, requires a vertical length at least $h_i + h_{i+1}$.

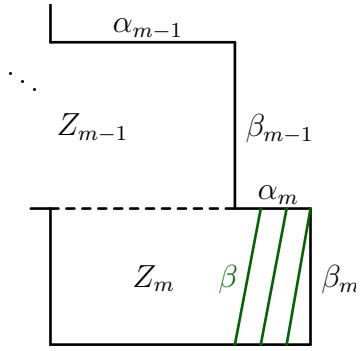

Figure 18: Example of β with co-slope $\frac{1}{3\Phi}$. Here, $\mathrm{Int}(\alpha_m, \beta) = 3$ with an intersection at the singularity.

In particular, $K(\infty, \frac{1}{k\Phi}) \geq \frac{1}{\Phi l_m^2}$, and the reversed inequality holds since the other saddle connections of direction $d' = \frac{1}{k\Phi}$ do not intersect α_m, and as seen in Case 1.1 the intersection of any β with α_i, $i < m$, gives a lower ratio. Consequently,

$$(\spadesuit)\ \forall k \in \mathbb{N}^* \cup \{\infty\},\ K(\infty, \frac{1}{k\Phi}) = \frac{1}{\Phi l_m^2}.$$

Case 1.2.ii. In the second case, the geodesic β is not contained in the horizontal cylinder Z_m. As such, β has a vertical length at least the length of β_{m-1}, that is $h_{m-1} = (\Phi^3 - 2\Phi) l_m$.

(1.2.ii.a) If $\mathrm{Int}(\alpha_m, \beta) = 0$ or 1, we directly have

$$\frac{\mathrm{Int}(\alpha_m, \beta)}{\alpha_m \wedge \beta} \leq \frac{1}{(\Phi^3 - 2\Phi) l_m^2},$$

with equality if and only if $\mathrm{Int}(\alpha_m, \beta) = 1$ and the vertical length of β is exactly h_{m-1}. In particular, β is contained in the horizontal cylinder Z_{m-1}

and up to an horizontal twist, its direction is $d' = 0$ or $d' = \pm\frac{\Phi^2-1}{\Phi^3-2\Phi}$ (see Figure 16). The case $d' = 0$ is an instance of case ♠ and has already been dealt with. The case $d' = \pm\frac{\Phi^2-1}{\Phi^3-2\Phi}$ is exactly case ♦. Further, taking the diagonal saddle connections γ and γ' of Figure 16 of respective holonomy vectors $\begin{pmatrix}\Phi^2-1\\ \Phi\end{pmatrix} l_m$ and $\begin{pmatrix}1\\ \Phi\end{pmatrix} l_m$ which intersect once at the singularity, we get:

$$\frac{\mathrm{Int}(\gamma,\gamma')}{\gamma\wedge\gamma'} = \frac{1}{(\Phi^3-2\Phi)l_m^2} = K(\infty, \frac{\Phi^2-1}{\Phi^3-2\Phi}),$$

This is due to the fact that the pair of directions $(\frac{1}{\Phi}, \Phi - \frac{1}{\Phi})$ is the image of the pair $(\infty, \frac{\Phi^2-1}{\Phi^3-2\Phi})$ by the diagonal action of the matrix $T_V R$ which belongs to the (unoriented) Veech group. In particular:

$$K(\frac{1}{\Phi}, \Phi - \frac{1}{\Phi}) = K(\infty, \frac{\Phi^2-1}{\Phi^3-2\Phi}).$$

(1.2.ii.b) Otherwise, β intersects α_m outside the singularity and is not contained in the horizontal cylinder Z_m. In this case, we show:

Lemma 4.9. *Assume β intersects α_m outside the singularity and is not contained in the horizontal cylinder Z_m. Then*

$$\frac{\mathrm{Int}(\alpha_m,\beta)}{\alpha_m\wedge\beta} < \frac{1}{(\Phi^3-2\Phi)l_m^2}.$$

Proof. Let c denote the co-slope of β. The assumption ensures that $c \neq \frac{1}{k\Phi}$. Up to an horizontal twist, we can also assume that $c \in]-\frac{1}{\Phi}, \Phi - \frac{1}{\Phi}[$. Finally, up to a symmetry with respect to the vertical axis, we can further assume $c > 0$, giving:

$$c \in]0, \Phi - \frac{1}{\Phi}[\setminus\{\frac{1}{k\Phi}, k \in \mathbb{N}^* \cup \{\infty\}\}$$

1. Let us first study the case $\frac{1}{\Phi} < c < \Phi - \frac{1}{\Phi}$. Under this assumption, β has to vertically go through the small horizontal cylinder Z_m before any non singular intersection with α_m and vertically go through Z_{m-1} after each non-singular intersection with α_m (see Figure 19), so that if we denote by p the number of non singular intersections between α_m and β we get

$$l(\beta)\sin\theta \geq p(h_m + (h_m + h_{m-1}))$$

where θ is the angle between the horizontal and the direction of β, so that $l(\beta)\sin\theta$ is the vertical length of β.
Now, adding the possible singular intersection, we deduce that

$$\begin{aligned}\frac{\mathrm{Int}(\alpha_m,\beta)}{\alpha_m\wedge\beta} &\leq \frac{p+1}{p(h_m + (h_m + h_{m-1}))l_m}\\ &= \frac{p+1}{p\Phi^3}\cdot\frac{1}{l_m^2}.\end{aligned}$$

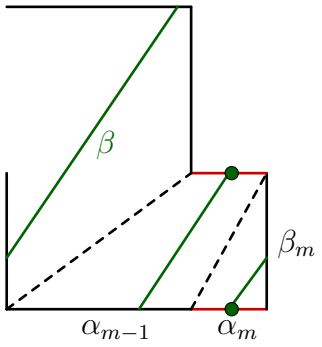

Figure 19: If the co-slope of β lies between $\frac{1}{\Phi}$ and $\Phi - \frac{1}{\Phi}$, then a non-singular intersection with α_m requires a vertical length at least $h_m + (h_m + h_{m-1})$.

(Recall that $h_m = \Phi l_m$ and $h_{m-1} = (\Phi^3 - 2\Phi) l_m$.)
The last quantity is maximal for $p = 1$, so that

$$\frac{\mathrm{Int}(\alpha_m, \beta)}{\alpha_m \wedge \beta} \leq \frac{2}{\Phi^3} \cdot \frac{1}{l_m^2} < \frac{1}{\Phi^3 - 2\Phi} \cdot \frac{1}{l_m^2}$$

where the last inequality comes from $\Phi < 2$.

2. Now, assume $0 < c < \frac{1}{\Phi}$ and let $k \geq 0$ be such that $\frac{1}{(k+1)\Phi} < c < \frac{1}{k\Phi}$. Let $p \geq 1$ denote the number of times the curve β crosses the small vertical cylinder C_m, that is the number of connected components of $\beta \cap C_m$. Then β crosses C_{m-1} at most once fewer, say $p' \geq 1$ times with $p' \geq p - 1$. Moreover, the assumption on the co-slope gives that for each crossing of C_m the curve β intersects at most $k + 1$ times α_m and for each crossing of C_{m-1} it intersects at least k times α_{m-1} (see Figure 20). This gives that :

$$\mathrm{Int}(\alpha_m, \beta) \leq s^{\circ}_{max} := p(k+1) + 1$$

(where the added intersection stands for the possible singular intersection). In fact, this estimate can be improved in the cases $p' = p$ and $p' = p - 1$ as follows:

- ★ If $p' = p$, the curve β has to either start or end at a vertex of C_m, so that either the first or the last crossing of C_m has only k intersections with α_m instead of $k + 1$. Hence,

$$\mathrm{Int}(\alpha_m, \beta) \leq s^{\star}_{max} := k(p+1) = (k+1)p - 1 + 1.$$

- ▲ If $p' = p - 1$ (so that $p \geq 2$), the curve β has to both start and end at a vertex of C_m. The same argument shows:

$$\mathrm{Int}(\alpha_m, \beta) \leq s^{\Delta}_{max} := (k+1)p - 1 = (k+1)p - 2 + 1.$$

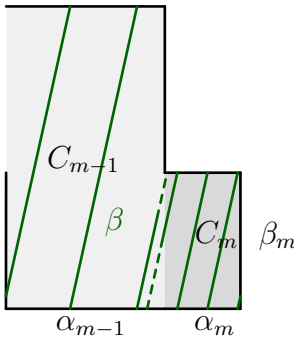

Figure 20: A portion of the curve β with co-slope $\frac{1}{3\Phi} < c < \frac{1}{2\Phi}$. Each time β crosses the cylinder C_m, it gives at most $k+1=3$ intersections with α_m and it is followed by a crossing of C_{m-1}, giving at least $k=2$ intersections with α_{m-1}.

Concerning the lengths, cutting β at each intersection with α_m and α_{m-1} helps us notice that:

- (i) Before any non-singular intersection with α_m, there is a vertical length at least h_m.
- (ii) Before any non-singular intersection with α_{m-1}, there is a vertical length at least $h_m + h_{m-1}$, except maybe the first intersection with α_{m-1} for which there is a vertical length a least h_{m-1} (but note that this case arises only if α starts at a bottom vertex of Z_{m-1}, in particular this cannot happen for $p' = p-1$).
- (iii) We further have to count a vertical length h_m for β to reach the singularity after the last intersection with either α_m or α_{m-1}.

In particular, letting $s := Int(\alpha_m, \beta) \geq 2$ (so that there are at least $s-1$ non-singular intersections), we have :

$$\begin{aligned} l(\beta)\sin\theta &\geq (s-1)h_m + (kp'-1)(h_m+h_{m-1}) + h_{m-1} + h_m \\ &= kp'(h_m+h_{m-1}) + (s-1)h_m, \end{aligned}$$

and for $p' = p-1$, we can replace $kp'-1$ by kp' as remarked in (ii).

$$\begin{aligned} l(\beta)\sin\theta &\geq (s-1)h_m + kp'(h_m+h_{m-1}) + h_m \\ &= k(p-1)(h_m+h_{m-1}) + sh_m. \end{aligned}$$

In particular, the following inequalities holds:

$$\text{If } p' \geq p, \text{ then } \frac{\mathrm{Int}(\alpha_m,\beta)}{\alpha_m \wedge \beta} \leq \frac{s}{p'k(h_m+h_{m-1}) + (s-1)h_m} \cdot \frac{1}{l_m}$$

$$(\blacktriangle)\ \text{If } p' = p-1, \text{ then } \frac{\mathrm{Int}(\alpha_m,\beta)}{\alpha_m \wedge \beta} \leq \frac{s}{(p-1)k(h_m+h_{m-1}) + sh_m} \cdot \frac{1}{l_m}.$$

Now, since $k(h_m + h_{m-1}) > h_m$, for fixed k and p, the right part is maximal when s is maximal. Distinguishing cases ● ($p' \geq p+1$), ★ ($p' = p$) and ▲ ($p' = p-1$), we have:

- ● If $p' \geq p+1$, then $s_{max} = s^{\circ}_{max} = p(k+1)+1$ and

$$\begin{aligned}\frac{\mathrm{Int}(\alpha_m, \beta)}{\alpha_m \wedge \beta} &\leq \frac{p(k+1)+1}{p'k(\Phi^3 - \Phi) + p(k+1)\Phi} \cdot \frac{1}{l_m^2} \\ &\leq \frac{p(k+1)+1}{(p+1)k(\Phi^3 - \Phi) + p(k+1)\Phi} \cdot \frac{1}{l_m^2} \\ &= \frac{pk+p+1}{k((p+1)\Phi^3 - \Phi) + p\Phi} \cdot \frac{1}{l_m^2}\end{aligned}$$

(given that $h_m = \Phi l_m$ and $h_{m-1} = (\Phi^3 - 2\Phi) l_m$.)

To give an upper bound for this last quantity, it is convenient to use the following lemma which will be used several times along the proof:

Lemma 4.10. *Let $a, b, c, d \in \mathbb{R}$. Assume the möbius transformation $f : x \mapsto \frac{ax+b}{cx+d}$ is defined for any $x \geq 1$. Then,*

- *if $ad - bc \geq 0$, then $\forall x \geq 1$, $f(x) \leq \lim_{x\to\infty} f(x) = \frac{a}{c}$.*
- *Otherwise, $\forall x \geq 1$, $f(x) \leq f(1) = \frac{a+b}{c+d}$.*

Proof. f is differentiable of derivative map $f'(x) = \frac{ad-bc}{(cx+d)^2}$. □

Since for any fixed $p \geq 1$ we have $p^2\Phi - (p+1)((p+1)\Phi^3 - \Phi) < (p+1)^2(\Phi - \Phi^3) < 0$, we can use Lemma 4.10 to conclude that the last quantity is maximal for $k = 1$, and it gives

$$\begin{aligned}\frac{\mathrm{Int}(\alpha_m, \beta)}{\alpha_m \wedge \beta} &\leq \frac{2p+1}{(p+1)(\Phi^3 - \Phi) + 2p\Phi} \cdot \frac{1}{l_m^2} \\ &= \frac{2p+1}{p(\Phi^3 + \Phi) + (\Phi^3 - \Phi)} \cdot \frac{1}{l_m^2}\end{aligned}$$

Similarly, given the inequality $2(\Phi^3 - \Phi) - (\Phi^3 + \Phi) < 0$, coming from $\Phi > 2\cos(\frac{\pi}{6}) = \sqrt{3}$, Lemma 4.10 shows that the last quantity is maximal for $p \to \infty$, and we have

$$\frac{\mathrm{Int}(\alpha_m, \beta)}{\alpha_m \wedge \beta} = \frac{2}{\Phi^3 + \Phi} \cdot \frac{1}{l_m^2} < \frac{1}{\Phi^3 - 2\Phi} \cdot \frac{1}{l_m^2},$$

where the last inequality comes from $\Phi < 2$.

★ If $p' = p$, then $s_{max} = s^\star_{max} = p(k+1)$ and:

$$\begin{aligned}\frac{\mathrm{Int}(\alpha_m, \beta)}{\alpha_m \wedge \beta} &\leq \frac{p(k+1)}{pk(\Phi^3 - \Phi) + (p(k+1)-1)\Phi} \cdot \frac{1}{l_m^2} \\ &= \frac{p(k+1)}{p(k\Phi^3 + \Phi) - \Phi} \cdot \frac{1}{l_m^2}\end{aligned}$$

Similarly, for fixed k the last quantity is maximal for $p = 1$, giving

$$\begin{aligned}\frac{\mathrm{Int}(\alpha_m, \beta)}{\alpha_m \wedge \beta} &\leq \frac{k+1}{k(\Phi^3 - \Phi) + k\Phi} \cdot \frac{1}{l_m^2} \\ &= \frac{k+1}{k\Phi^3} \cdot \frac{1}{l_m^2} < \frac{2}{\Phi^3} \cdot \frac{1}{l_m^2} < \frac{1}{\Phi^3 - 2\Phi} \cdot \frac{1}{l_m^2}.\end{aligned}$$

▲ Finally, if $p' = p - 1$, we have $s_{max} = s^\Delta_{max} = p(k+1) - 1$ and:

$$\begin{aligned}\frac{\mathrm{Int}(\alpha_m, \beta)}{\alpha_m \wedge \beta} &\leq \frac{p(k+1) - 1}{(p-1)k(\Phi^3 - \Phi) + (p(k+1)-1)\Phi} \cdot \frac{1}{l_m^2} \\ &= \frac{p(k+1) - 1}{p(k\Phi^3 + \Phi) - k\Phi^3 + (k-1)\Phi} \cdot \frac{1}{l_m^2}\end{aligned}$$

Using the inequality $(k+1)((k-1)\Phi - k\Phi^3) + k\Phi^3 + \Phi = k^2(\Phi - \Phi^3) < 0$ and Lemma 4.10, we see that for fixed $k \geq 1$, the last quantity is maximal for p minimal, that is $p = 2$ since $p' = p - 1$ should be at least one. In particular

$$\begin{aligned}\frac{\mathrm{Int}(\alpha_m, \beta)}{\alpha_m \wedge \beta} &\leq \frac{2k+1}{k(\Phi^3 - \Phi) + (2k+1)\Phi} \cdot \frac{1}{l_m^2} \\ &= \frac{2k+1}{k(\Phi^3 + \Phi) + \Phi} \cdot \frac{1}{l_m^2}\end{aligned}$$

which, using again Lemma 4.10, is shown to be minimal for $k = 1$, so that

$$\frac{\mathrm{Int}(\alpha_m, \beta)}{\alpha_m \wedge \beta} < \frac{3}{\Phi^3 + 2\Phi} \cdot \frac{1}{l_m^2} < \frac{1}{\Phi^3 - 2\Phi} \cdot \frac{1}{l_m^2},$$

where the last inequality comes from $\Phi < 2$.

This concludes the proof of Lemma 4.9. □

Case 2: d represents the vertical cusp. Up to the action by an element of the Veech group, we can assume that α is one of the β_j, $j \in [\![1, m]\!]$. We first study the case $\alpha = \beta_j$ for $j < m$.

Case 2.1: $\alpha = \beta_j$ for $j < m$.

Lemma 4.11. *Assume $d' \notin \{\frac{1}{k\Phi}, k \in \mathbb{N} \cup \{\infty\}\}$. For any $j < m$,*

$$\frac{\mathrm{Int}(\beta_j, \beta)}{\beta_j \wedge \beta} < \frac{1}{(\Phi^3 - 2\Phi)} \cdot \frac{1}{l_m^2}$$

Proof. First notice that if β has horizontal length l_m, then its direction is $\frac{1}{k\Phi}$ for a given k. In particular the assumption on d' ensures that β has horizontal length at least than l_{m-1}. Further, any non-singular intersection with β_j for $j < m$ requires an horizontal length $l_j + l_{j-1}$ (see Figure 21). This gives, for $j < m$,

$$\beta_j \wedge \beta \geq h_j \max((l_j + l_{j-1})(\mathrm{Int}(\beta_j, \beta) - 1), l_{m-1}).$$

In particular,

(i) If $\mathrm{Int}(\beta_j, \beta) \leq 1$, we use $\beta_j \wedge \beta \geq h_j l_{m-1}$ to get

$$\frac{\mathrm{Int}(\beta_j, \beta)}{\beta_j \wedge \beta} \leq \frac{1}{l_{m-1} h_j} \leq \frac{1}{l_{m-1} h_{m-1}}.$$

Then, given that $l_{m-1} = (\Phi^2 - 1) l_m$ and $h_{m-1} = (\Phi^3 - 2\Phi) l_m$, we draw:

$$\frac{\mathrm{Int}(\beta_j, \beta)}{\beta_j \wedge \beta} \leq \frac{1}{(\Phi^3 - 2\Phi)(\Phi^2 - 1) l_m^2} < \frac{1}{(\Phi^3 - 2\Phi)} \cdot \frac{1}{l_m^2}$$

(ii) Otherwise, we use $\beta_j \wedge \beta \geq h_j (l_j + l_{j-1})(\mathrm{Int}(\beta_j, \beta) - 1)$ to obtain:

$$\frac{\mathrm{Int}(\beta_j, \beta)}{\beta_j \wedge \beta} \leq \frac{2}{h_j (l_j + l_{j-1})}.$$

Since $2 l_{m-1} \leq 2 l_j < (\Phi^2 - 1) l_j = l_{j-1}$, we deduce that

$$\frac{\mathrm{Int}(\beta_j, \beta)}{\beta_j \wedge \beta} \leq \frac{1}{h_j l_{m-1}} \leq \frac{1}{l_{m-1} h_{m-1}} < \frac{1}{(\Phi^3 - 2\Phi)} \cdot \frac{1}{l_m^2}.$$

□

Case 2.2: $\alpha = \beta_m$. In this case α is homologous to a non singular geodesic so there is no non singular intersection. The first intersection with β_m requires a horizontal length at least l_m while all the following intersections require a length $l_{m-1} + l_m$. In particular, either β stays in the vertical cylinder C_m and the co-slope is $\frac{1}{k\Phi}$ for $k \in \mathbb{N} \cup \{\infty\}$ (case ♠), or there are at least two intersections and

$$\frac{\mathrm{Int}(\beta_m, \beta)}{\beta_m \wedge \beta} \leq \frac{2}{h_m (2 l_m + l_{m-1})} = \frac{2}{\Phi(\Phi^2 + 1)} \cdot \frac{1}{l_m^2} < \frac{1}{\Phi^3 - 2\Phi} \cdot \frac{1}{l_m^2}.$$

where the last inequality comes from $\Phi < 2$. This concludes the proof of Proposition 4.7.

□

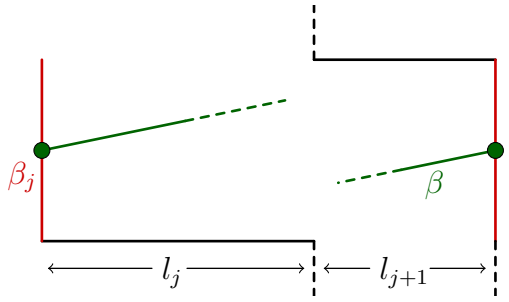

Figure 21: Any non-singular intersection with β_j requires a horizontal length at least $l_j + l_{j+1}$.

5 Proof of Theorem 1.1

In this section, we finally prove our main result. More precisely, we show

Theorem 5.1. *For any $X \in \mathcal{T}_n$, we have*

$$\mathrm{KVol}(X) = \mathrm{Vol}(X) K(\infty, \frac{1}{\Phi}) \cdot \frac{1}{\cosh(\mathrm{dist}_{\mathbb{H}^2}(X, \Gamma_n \cdot \mathcal{G}_{max}))} \tag{9}$$

Recall that $\mathcal{G}_{max} = \bigcup_{k \in \mathbb{N}^* \cup \{\infty\}} \gamma_{\infty, \pm \frac{1}{k\Phi}}$, and notice that the constant K_0 given in the statement of Theorem 1.1 is now explicitely determined by $K_0 = \mathrm{Vol}(X) K(\infty, \frac{1}{\Phi})$.

We begin this section by giving an overview of the geometric ideas behind the proof.

5.1 Geometric interpretation of Proposition 4.4

Following §7.2 of [BLM22], we first give a geometric interpretation of Equation (8) (see Proposition 4.4), which we restate here for the reader's convenience:

$$\mathrm{KVol}(X) = \mathrm{Vol}(X) \cdot \sup_{\substack{d, d' \in \mathcal{P} \\ d \neq d'}} K(d, d') \cdot \sin \theta(X, d, d').$$

Recall that $\mathcal{P}$ is the set of periodic directions on the staircase model $\mathcal{S}_n$.

Given a pair of distinct periodic directions (d, d'), its associated geodesic $\gamma_{d,d'}$ on $\mathbb{H}^2$ gives a projected geodesic on the hyperbolic surface $\mathbb{H}^2/\Gamma_n$. In the fundamental domain $\mathcal{T}_n$, it gives a set of geodesics formed by all the images of $\gamma_{d,d'}$ by an element of Γ_n. By Remark 4.5, all pairs of directions in $\Gamma_n^{\pm} \cdot (d, d')$ give the same value for $K(\cdot, \cdot)$. This amounts to saying that the corresponding geodesic trajectory on the surface $\mathbb{H}^2/\Gamma_n$ has a well defined associated constant, $K(d, d')$. Now, given a point $X \in \mathbb{H}^2/\Gamma_n$, we can look at the minimal distance r from X to the geodesic trajectory associated with (d, d'). Proposition 4.2 gives that for

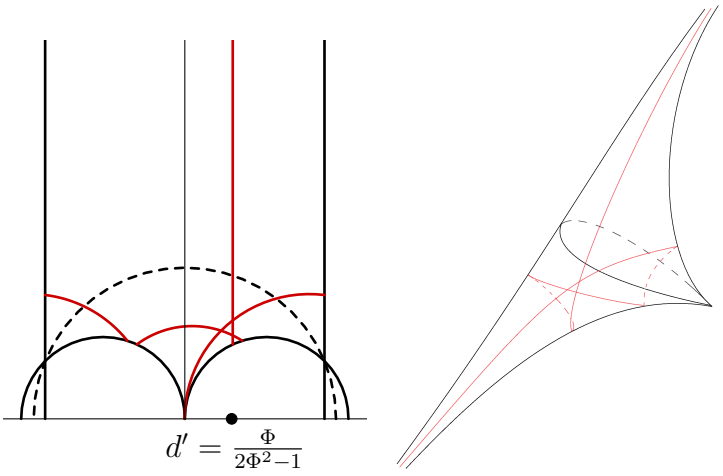

Figure 22: The geodesic $\gamma_{\infty,\frac{\Phi}{2\Phi^2-1}}$ its images by the Veech group intersecting the fundamental domain $\mathcal{T}_n$. On the right, the same geodesics on the surface $\mathbb{H}^2/\Gamma_n$.

a pair of saddle connections α and β on X of respective directions d and d' (in the sense of Definition 4.1), we have the sharp inequality:

$$\frac{\mathrm{Int}(\alpha,\beta)}{l(\alpha)l(\beta)} \leq K(d,d') \times \frac{1}{\cosh r}.$$

Examples of geodesic trajectories for $d = \infty$ and $d' = \frac{1}{\Phi}, \frac{1}{2\Phi}$ and $\frac{1}{3\Phi}$ are depicted in Figure 1 of the introduction, as well as in Figure 22 for $d' = \frac{\Phi}{2\Phi^2-1}$.

Using this interpretation, we can prove Theorem 5.1 by showing that for every pair of distinct periodic directions (d,d') and any $X \in \mathcal{T}_n$ (or, by symmetry, for any $X \in \mathcal{T}_{n+} = \{X = x+iy \in \mathcal{T}_n, x \geq 0\}$) we have:

$$K(d,d')\sin\theta(X,d,d') \leq \max_{k\in\mathbb{N}^*}\{K(\infty,\frac{1}{k\Phi})\sin\theta(X,\infty,\frac{1}{k\Phi})\} \qquad (\clubsuit)$$

The constant $K(\infty,\frac{1}{k\Phi})$ being maximal among all possible constants $K(d,d')$, Equation ($\clubsuit$) holds for surfaces X close to $\Gamma_n \cdot \mathcal{G}_{max}$. More precisely, in §5.2, we use Proposition 4.7 to show that ($\clubsuit$) holds in the domain $\mathcal{R}_+ = \{X = x+iy \in \mathcal{T}_{n+}, y \geq x - \frac{1}{\Phi}\}$ (Lemma 5.2 and Figure 23).

Then, it remains to deal with surfaces outside $\mathcal{R}_+$ (which are, in some sense, surfaces close to the regular n-gon X_n). This latter case is explained in §5.3 and requires use of the machinery of [BLM22, §7], along with Corollary 4.6 and Proposition 4.7.

5.2 The case of surfaces close to $\Gamma_n \cdot \mathcal{G}_{max}$

With the above geometric interpretation, we deduce that for surfaces close to the geodesic trajectories associated to the directions $(\infty, \frac{1}{k\Phi})$, $k \in \mathbb{N}^* \cup \{\infty\}$ (having maximal $K(\cdot,\cdot)$), KVol is achieved by pairs of saddle connections in directions $d = \infty$ and $d' = \frac{1}{k\Phi}$, and Equation (♣) holds. More precisely, we have:

Lemma 5.2. *For any $X \in \mathcal{R}_+ = \{X = x + iy \in \mathcal{T}_{n+}$ with $y \geq x - \frac{1}{\Phi}\}$, Equation (♣) holds.*

Recall that because of the symmetry of KVol with respect to the reflection on the vertical axis, we can assume $X \in \mathcal{T}_{n+} := \{X = x + iy \in \mathcal{T}_n, x \geq 0\}$.

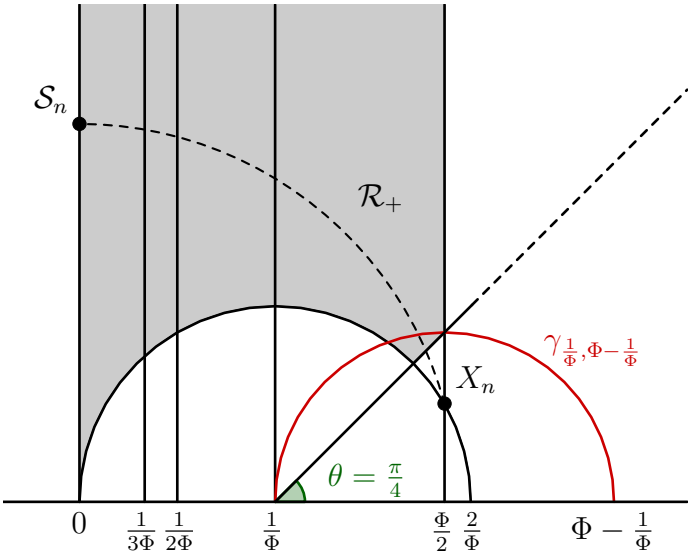

Figure 23: The region $\mathcal{R}_+$ in the right part of the fundamental domain ${\mathcal{T}_n}^+$ and the geodesic $(\frac{1}{\Phi}, \Phi - \frac{1}{\Phi})$ for the case $n = 12$.

Proof. By Proposition 4.7, Equation (♣) holds for any $X \in {\mathcal{T}_n}^+$ such that there is a $k \in \mathbb{N}^* \cup \{\infty\}$ with

$$\sin\theta(X, \infty, \frac{1}{k\Phi}) \geq \frac{1}{\Phi^2 - 2}. \tag{10}$$

Since $\dfrac{1}{\Phi^2 - 2} \leq \dfrac{1}{\Phi_8^2 - 2} = \dfrac{\sqrt{2}}{2} = \sin\dfrac{\pi}{4}$, we directly have that the above condition is verified for $X \in \{Y \in {\mathcal{T}_n}^+, \exists k \in \mathbb{N}^* \cup \{\infty\}, \theta(Y, \infty, \frac{1}{k\Phi}) \geq \frac{\pi}{4}\}$. One verifies that this set is exactly $\mathcal{R}_+$. □

Remark 5.3. In fact, $\mathcal{R}_+ = {\mathcal{T}_n}^+$ for $m = 2$, which finishes the proof in the case of the octagon. However, this is no longer the case for $m \geq 3$.

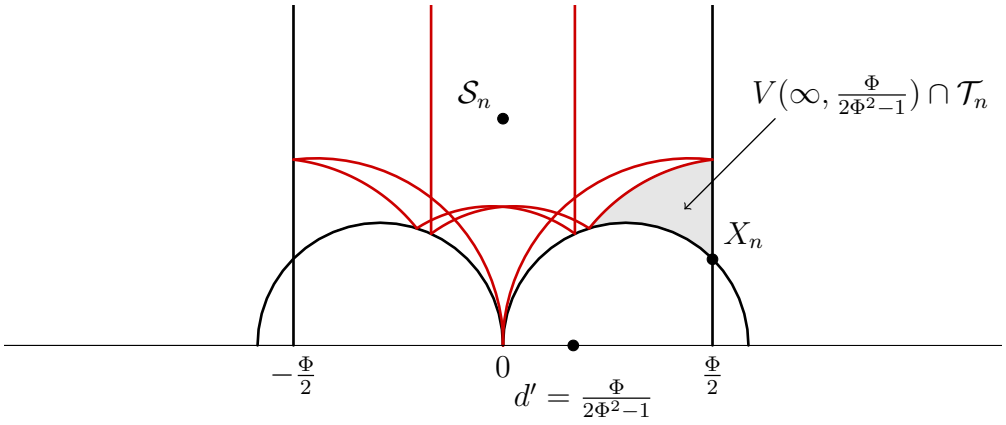

Figure 24: The geodesics of $\Gamma_n^{\pm} \cdot \gamma_{\infty, \frac{\Phi}{2\Phi^2-1}}$ intersecting the fundamental domain $\mathcal{T}_n$, and the domain $V(\infty, \frac{\Phi}{2\Phi^2-1}) \cap \mathcal{T}_n$.

5.3 The case of surfaces close to X_n

It remains to deal with surfaces away from geodesics associated with directions ∞ and $\frac{1}{k\Phi}$. In a way, these surfaces are close to the regular n-gon X_n. To this end we make the following definition (which can also be found in [BLM22, §7.2]):

Definition 5.4. Given a pair of distinct periodic directions (d, d') and its associated geodesic $\gamma_{d,d'}$ on $\mathbb{H}^2$, we denote by $V(d, d')$ the connected component of $\mathbb{H}^2 \backslash (\Gamma_n^{\pm} \cdot \gamma_{d,d'})$ containing X_n.

As an example, the domain $V(\infty, d')$ with $d' = \frac{\Phi}{2\Phi^2-1}$ is drawn in Figure 24.

Remark 5.5. If a geodesic of $\Gamma_n^{\pm} \cdot \gamma_{d,d'}$ passes through X_n, then $V(d, d')$ is not well defined. For convenience, we set $V(d, d') = \{X_n\}$ as in this case we automatically have:

$$K(d, d') \leq K(\infty, \frac{1}{\Phi}) \sin \theta(X_n, \infty, \frac{1}{\Phi})$$

and since X_n is the furthest point away from the set of geodesics $\mathcal{G}_{max}$, we have for any surface $X \in \mathcal{T}_n$:

$$K(d, d') \sin \theta(X, d, d') \leq K(d, d') \leq K(\infty, \frac{1}{\Phi}) \sin \theta(X_n, \infty, \frac{1}{\Phi}).$$

With this definition, the proof of Lemmas 7.6 and 7.7 of [BLM22, §7.2] generalizes to our setting and gives:

Lemma 5.6. *Let (d_0, d_0') be a pair of distinct periodic directions. Assume that Equation (♣) holds for any pair of directions (d, d') whose associated geodesic lie in the boundary of the domain $V(d_0, d_0')$. Then the same inequality is true for (d_0, d_0').*

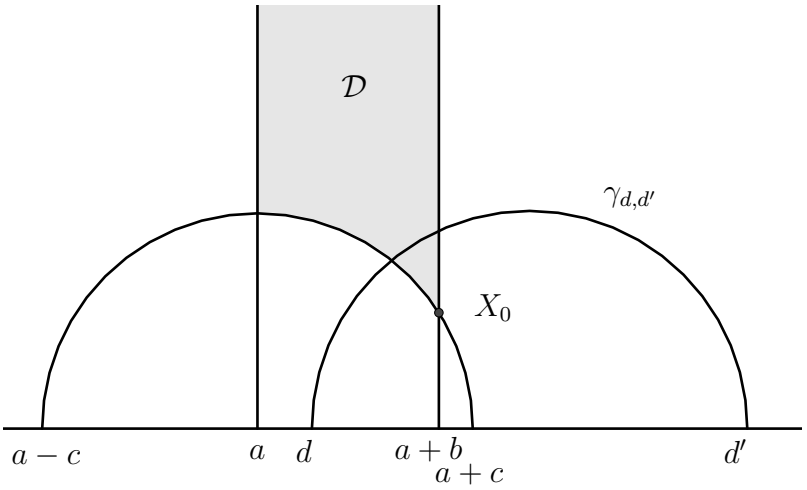

Figure 25: The domain $\mathcal{D}$ of Proposition 5.8.

Furthermore, a pair of directions (d, d'), $d < d'$ whose associated geodesic lies in the boundary of the domain $V(d_0, d_0') \cap \mathcal{T}_{n+}$ has to satisfy $d' + d \geq \Phi$.

In particular, it suffices to prove Equation (♣) for pairs of directions (d, d') with $d + d' \geq \Phi$. This relies on the sinus comparison techniques of [BLM22, §7.3].

Proposition 5.7. *Let (d, d') with $d + d' \geq \Phi$ and $X = x + iy \in \mathcal{T}_n$ inside the half disk defined by the geodesic $\gamma_{\frac{1}{\Phi}, \Phi - \frac{1}{\Phi}}$. We have*

$$K(d, d') \sin \theta(X, d, d') \leq K(\infty, \frac{1}{\Phi}) \sin \theta(X, \infty, \frac{1}{\Phi}).$$

This condition is verified in particular for $X \in \mathcal{T}_n \backslash \mathcal{R}_+$.

Proof of Proposition 5.7. We distinguish two cases:

1. In the case $d \geq \frac{1}{\Phi}$, we use Proposition 7.8 of [BLM22] which can be stated more generally as:

   Proposition 5.8. *Let $a \in \mathbb{R}$, $b > 0$, and $c \geq b$. Let $\mathcal{D} \subset \mathbb{H}^2$ be the domain enclosed by the geodesics $\gamma_{a,\infty}$, $\gamma_{a+b,\infty}$ and $\gamma_{a-c,a+c}$, and X_0 be the right corner of the domain $\mathcal{D}$, as in Figure 25. Then for any (d, d') with $a \leq d \leq a + b \leq d'$ such that $\gamma_{d,d'}$ intersect the domain $\mathcal{D}$, the function*

   $$F_{(d,d')} : X \in \mathcal{D} \mapsto \frac{\sin \theta(X, \infty, a)}{\sin \theta(X, d, d')}$$

   is minimal at X_0 on the domain $\mathcal{D}$.

In our setting, we set $a = \frac{1}{\Phi}$, $b = \frac{\Phi}{2} - \frac{1}{\Phi}$ and $c = \frac{1}{\Phi}$ and it gives that for any (d, d') with $\frac{1}{\Phi} \leq d \leq \frac{\Phi}{2} \leq d'$, the function

$$F_{(d,d')} : X \mapsto \frac{\sin\theta(X, \infty, \frac{1}{\Phi})}{\sin\theta(X, d, d')}$$

is minimal at X_n on the domain $\mathcal{D} = \{X = x + iy \in \mathcal{T}_n \text{ with } x \geq \frac{1}{\Phi}\}$.
In particular, since by Corollary 4.6

$$\forall (d, d'),\ K(d, d') \sin\theta(X_n, d, d') \leq K(\infty, \frac{1}{\Phi}) \sin\theta(X_n, \infty, \frac{1}{\Phi})$$

we deduce that for all $X \in \{X = x + iy \in \mathcal{T}_n \text{ with } x \geq \frac{1}{\Phi}\}$ and (d, d') with $\frac{1}{\Phi} \leq d \leq \frac{\Phi}{2} \leq d'$, we have

$$K(d, d') \sin\theta(X, d, d') \leq K(\infty, \frac{1}{\Phi}) \sin\theta(X, d, d').$$

2. Else, $d < \frac{1}{\Phi}$ so that $d' > \Phi - \frac{1}{\Phi}$. In this case, for any pair of directions (d, d') not in $\Gamma \cdot \mathcal{G}_{max}$ and such that $d \leq \frac{1}{\Phi}$ and $d' \geq \Phi - \frac{1}{\Phi}$, and for all $X \in \mathcal{R}_+$, we have $\sin\theta(X, d, d') \leq \sin\theta(X, \frac{1}{\Phi}, \Phi - \frac{1}{\Phi})$ so that

$$\begin{aligned} K(d, d') \sin\theta(X, d, d') &\leq K(d, d') \sin\theta(X, \frac{1}{\Phi}, \Phi - \frac{1}{\Phi}) \\ &\leq K(\frac{1}{\Phi}, \Phi - \frac{1}{\Phi}) \sin\theta(X, \frac{1}{\Phi}, \Phi - \frac{1}{\Phi}) \quad \text{(by Proposition 4.7)} \\ &\leq K(\infty, \frac{1}{\Phi}) \sin\theta(X, \infty, \frac{1}{\Phi}) \quad \text{(by case 1.)} \end{aligned}$$

This concludes the proof.

□

6 Proof of Theorem 1.4

In the case where $n \equiv 2 \mod 4$, saddle connections are not necessarily closed anymore, and it is no longer possible to use techniques from Sections 4 and 5. However, we can still show that KVol is bounded on the Teichmüller disk of X_n. In §6.1, we extend a boundedness criterion of [BLM22, §3] to the case of multiple singularities. In §6.2, we use this criterion to show that KVol is bounded on the Teichmüller disk of the regular n-gon.

6.1 Boundedness criterion for multiple singularities

In this paragraph, we show Theorem 1.5 which extends the boundedness criterion of [BLM22] to the case of translation surfaces with multiple singularities.

Theorem 1.5. KVol is bounded on the Teichmüller disk of a Veech surface X if and only if there are no intersecting closed curves α and β on X such that $\alpha = \alpha_1 \cup \cdots \cup \alpha_k$ and $\beta = \beta_1 \cup \cdots \cup \beta_l$ are unions of parallel saddle connections (that is all saddle connections $\alpha_1, \ldots, \alpha_k, \beta_1, \ldots, \beta_l$ have the same direction).

Proof. First, notice that if there exist a pair (α, β) of parralel closed curves, then applying the Teichmüller geodesic flow in their common direction make the length of both α and β go to zero, while the interserction remain unchanged. In particular

$$\mathrm{KVol}(g_t \cdot X) \to +\infty \text{ as } t \to +\infty.$$

Conversely, let X be a Veech surface, which we assume to be of unit area. Recall that for such a surface, the "no small triangle condition" of [Vor96] (see also [SW10]) gives a constant $A > 0$ such that for any two saddle connections α and β, the inequality $|\alpha \wedge \beta| \geq A$ holds. Further, the constant A does not depend on the choice of the surface in the Teichmüller disk of X.

Now, let α be a saddle connection in a periodic direction. The Veech surface X decomposes into cylinders in the direction of α. Let h be the smallest height of the cylinders. For any saddle connection β which is not parallel to α, β has at least a vertical length h between each non-singular intersection with α, plus a vertical length at least h before the first non-singular intersection, and after the last non-singular intersection with α. In particular, for any saddle connection β having at least one non-singular intersection with α, we have:

$$h(\beta) \geq h(|\alpha \cap \beta| + 1)$$

where $h(\beta) = l(\beta) \sin angle(\alpha, \beta)$. In fact, if β does not intersect α non-singularly then the above inequality still holds, as it becomes $h(\beta) \geq h$ which is true as long as β is not parallel to α. Finally, since $h(\beta) \leq l(\beta)$, we conclude that :

$$\frac{|\alpha \cap \beta| + 1}{l(\alpha) l(\beta)} \leq \frac{1}{l(\alpha) h} \leq \frac{1}{A}.$$

The last inequalty comes from the fact that $l(\alpha)h = \alpha \wedge \beta_0 \geq A$ for a saddle connection β_0 which stays inside the cylinder of height h.

Next, take α and β two simple closed curves decomposed as an union of saddle connections $\alpha = \alpha_1 \cup \cdots \cup \alpha_k$ and $\beta = \beta_1 \cup \cdots \cup \beta_l$, and assume that $\alpha_1, \ldots, \alpha_k, \beta_1, \ldots, \beta_l$ are not all parallel. Then,

$$\mathrm{Int}(\alpha, \beta) \leq \Big(\sum_{\substack{1 \leq i \leq k \\ 1 \leq j \leq l}} |\alpha_i \cap \beta_j| \Big) + s$$

where $s \leq \min(k, l)$ denotes the number of common singularities between α and β. It should be noted that if $\alpha_i = \beta_j$, we set $|\alpha_i \cap \beta_j| = 0$.

Now, since saddle connections are not all parallel, there is at least $\min(k,l)$ pairs (i,j) such that α_i and β_j are not parallel, and we get

$$\begin{aligned}\mathrm{Int}(\alpha,\beta) &\leq \Big(\sum_{\substack{1\leq i\leq k\\ 1\leq j\leq l}} |\alpha_i\cap\beta_j|\Big)+s\\ &\leq \sum_{\substack{i,j\\ \alpha_i \text{ and } \beta_j \text{ non-parallel}}} (|\alpha_i\cap\beta_j|+1)\\ &\leq \sum_{\substack{i,j\\ \alpha_i \text{ and } \beta_j \text{ non-parallel}}} \frac{1}{A}\times l(\alpha_i)l(\beta_j)\\ &\leq \frac{1}{A}l(\alpha)l(\beta).\end{aligned}$$

This gives the required boundedness result

$$\mathrm{KVol}(X)\leq\frac{1}{A}.$$

□

6.2 Intersection of parallel curves on X_n, $n\equiv 2 \mod 4$

In this paragraph, we go back to the regular n-gon for $n\equiv 2 \mod 4$ and we study the intersection $\mathrm{Int}(\alpha,\beta)$ in the case where α and β are union of parallel saddle connections. Up to the action of the Veech group, we can assume that α and β are either both horizontal or both vertical. We will work in the staircase model $\mathcal{S}$, as in Figure 26. Notice that in the horizontal direction, saddle connections go from one singularity to the other while saddle connections are closed curves in the vertical direction. In this latter case, it is easy to show:

Lemma 6.1 (Vertical curves)**.** *For every i,j,* $\mathrm{Int}(\beta_i,\beta_j)=0$

Proof. First, since β_m is homologous to a non-singular curve which do not intersect any of the β_j for $j<m$, we have $\mathrm{Int}(\beta_m,\beta_j)=0$.
Next, for any $j<m$ the curve $\beta_j+\beta_{j+1}$ is homologous to a non-singular curve and for all i, $\mathrm{Int}(\beta_j+\beta_{j+1},\beta_i)=0$ and hence $\mathrm{Int}(\beta_j,\beta_i)=-\mathrm{Int}(\beta_{j+1},\beta_i)$ and by induction $\mathrm{Int}(\beta_j,\beta_i)=\pm\mathrm{Int}(\beta_m,\beta_i)=0$. □

In the case where α (resp. β) is an horizontal curve made of two horizontal saddle connections α_{i_1} and α_{i_2} (resp. α_{j_1} and α_{j_2}) going from one singularity to the other and oriented such that the resulting curve $\alpha=\alpha_{i_1}\pm\alpha_{i_2}$ has a well defined orientation, we have:

Lemma 6.2 (Horizontal curves)**.** *In this setting,* $\mathrm{Int}(\alpha,\beta)=0$.

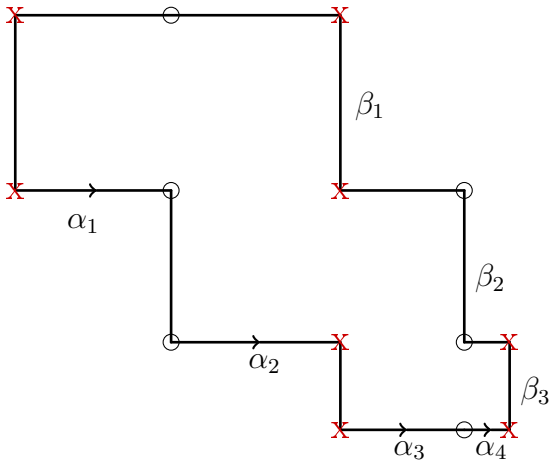

Figure 26: The staircase model associated with the 14-gon. The horizontal and the vertical direction represent the two cuspidal directions. Notice that vertical saddle connections are closed while horizontal saddle connections are not.

Proof. First notice that, given the orientation of the saddle connections α_i is from left to right as in Figure 26, the curve α has a well defined orientation if and only if $\alpha = \pm[\alpha_{i_1} + (-1)^{i_2-i_1-1}\alpha_{i_2}]$. In this case, we can write (assuming $i_1 < i_2$ for convenience)

$$\begin{aligned}\alpha &= \pm[(\alpha_{i_1} + \alpha_{i_1+1}) - (\alpha_{i_1+1} + \alpha_{i_1+2}) + \cdots + (-1)^{i_2-i_1-1}(\alpha_{i_2-1} + \alpha_{i_2})] \\ &= \pm \sum_{k=0}^{i_2-i_1-1} (-1)^k(\alpha_{i_1+k} + \alpha_{i_1+k+1}).\end{aligned}$$

Now, since the curves $\alpha_i + \alpha_{i+1}$ are closed curves homologous to core curve of horizontal cylinder, they are pairwise non-intersecting. Making the same decomposition for β gives directly $\mathrm{Int}(\alpha, \beta) = 0$. □

As a corollary, we can apply the criterion of Theorem 1.5 to deduce that KVol is bounded on the Teichmüller disk of the regular n-gon. In fact, a closer look at the proof of Theorem 1.5 gives the following explicit bound:

Corollary 6.3. *Let $n \geq 10$, $n \equiv 2 \mod 4$. For any surface X in the Teichmüller disk of the regular n-gon, and any closed curves α and β on X, we have:*

$$\frac{\mathrm{Int}(\alpha, \beta)}{l(\alpha)l(\beta)} \leq \frac{1}{\Phi l_m^2}.$$

References

[BLM22] Julien Boulanger, Erwan Lanneau, and Daniel Massart. Algebraic intersection in a family of veech surfaces. *arXiv:2110.14235*, 2022.

[CKM21a] Smail Cheboui, Arezki Kessi, and Daniel Massart. Algebraic intersection for translation surfaces in a family of Teichmüller disks. *Bull. Soc. Math. France*, 149(4):613–640, 2021.

[CKM21b] Smail Cheboui, Arezki Kessi, and Daniel Massart. Algebraic intersection for translation surfaces in the stratum $H(2)$. *C. R. Math. Acad. Sci. Paris*, 359:65–70, 2021.

[Mas22] Daniel Massart. A short introduction to translation surfaces, Veech surfaces, and Teichmüller dynamics. In *Surveys in geometry I*, pages 343–388. Springer, Cham, [2022] ©2022.

[MM14] Daniel Massart and Bjoern Muetzel. On the intersection form of surfaces. *Manuscr. Math.*, 143(1-2):19–49, 2014.

[Mon05] Thierry Monteil. On the finite blocking property. *Ann. Inst. Fourier*, 55(4):1195–1217, 2005.

[SU] John Smillie and Corinna Ulcigrai. Geodesic flow on the Teichmüller disk of the regular octagon cutting sequences and octagon continued fractions maps. In *Dynamical numbers. Interplay between dynamical systems and number theory.*

[SW10] John Smillie and Barak Weiss. Characterizations of lattice surfaces. *Invent. Math.*, 180(3):535–557, 2010.

[Vee89] W. A. Veech. Teichmüller curves in moduli space, Eisenstein series and an application to triangular billiards. *Invent. Math.*, 97(3):553–583, 1989.

[Vor96] Ya. B. Vorobets. Planar structures and billiards in rational polygons. *Russ. Math. Surv.*, 51(1):177–178, 1996.

[Wri16] Alex Wright. From rational billiards to dynamics on moduli spaces. *Bull. Amer. Math. Soc. (N.S.)*, 53(1):41–56, 2016.

[ZK76] A. N. Zemlyakov and A. B. Katok. Topological transitivity of billiards in polygons. *Math. Notes*, 18:760–764, 1976.

[Zor06] Anton Zorich. Flat surfaces. In *Frontiers in number theory, physics, and geometry. I*, pages 437–583. Springer, Berlin, 2006.